BUDAPEST UNIVERSITY OF TECHNOLOGY AND ECONOMICS

MSc in Chemical Engineering

THESIS PROJECT

"High-pressure phase equilibrium in a carbon dioxide-acetone-isopropanol ternary system: obtaining and analysing new datasets"
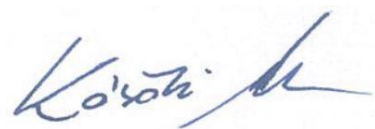
Written by Pablo Miranda Rey

Supervised by Márton Kőrösi, Department of Chemical and Environmental Process Engineering

Budapest, JANUARY 2022

Statement of the supervisor

I, Márton Kőrösi as supervisor, hereby declare that the thesis written by Pablo Miranda Rey, (Neptune code: PDQ13B) titled "High-pressure phase equilibrium in a carbon dioxide-acetone-isopropanol ternary system: obtaining and analysing new datasets"
is his own writing prepared under my supervision. I also declare that the thesis meets the formal and professional requirements of the Budapest University of Technology and Economics and those of the Faculty of Chemical Technology and Biotechnology, thus I support its submission.

Budapest, January 2022   Márton Kőrösi

Statement of the student

I, Pablo Miranda Rey (Neptun code: PDQ13B) as author of the thesis hereby declare that my thesis titled "High-pressure phase equilibrium in a carbon dioxide-acetone-isopropanol ternary system: obtaining and analysing new datasets" is my original writing and I have not plagiarised any other work. All third party materials including published and unpublished sources were referenced.

I acknowledge that the intellectual property rights of the methods used and the results of any research or development described in the thesis belong to the participating researchers and institutions/companies, thus their utilization or publication must not be initiated before the approval of all parties.

I also declare that during the preparation and writing the thesis I did not mislead my supervisor(s) and thesis advisor.

Budapest, January 2022   Pablo Miranda Rey

Contents

Acknowledgment

Abstract

This paper describes the work carried out to obtain and analyse the thermodynamic equilibrium dataset for the ternary mixture of carbon dioxide, acetone and isopropanol in a range of temperatures between 308.15 and 328.15 K and pressures between approximately 5 MPa and 14 MPa. The composition (molar fraction) of each compound was varied approximately in the ranges x_{CO_2} : $(0.7; 0.99)$; $x_{acetone}$: $(0.003; 0.24)$; x_{iPrOH} : $(0.001; 0.14)$ maintaining 3 different volumetric ratios of acetone/isopropanol: 1:1, 3:1 and 5:1. The measurements are based on the use of a static synthetic method in which the opacity and redissolution points are visually observed in a high-pressure, variable volume view-cell. The system has not been previously studied and therefore represents a novel contribution to high-pressure phase equilibria investigation.

The text can be divided into three main parts: (i) where the characteristics of supercritical fluids, especially supercritical CO_2 and the importance of phase equilibrium measurement in these systems are addressed; (ii) in which the experimental process carried out in the laboratory to obtain the data, as well as the equipment, the different existing phase equilibrium measurement methods and the one used in this work are explained; and (iii) in which the results obtained are analysed with the aim of predicting and understanding the behaviour of the system. To this end, a discussion of the raw data is conducted and the thermodynamic modelling using the Peng-Robinson and Soave-Redlich-Kwong equations of state is carried out.

Keywords: High-pressure phase equilibrium · Ternary system · Static methods · View cell · Carbon dioxide · Acetone · Isopropanol · Thermodynamic modelling.

List of Figures

List of Tables

List of Acronyms

BIP: binary interaction parameter

EOS: equation of state

GAS: gas antisolvent precipitation

HTL: hydrothermal liquefaction

HTC: hydrothermal carbonization

PR: Peng-Robinson

RESS: rapid expansion of supercritical solutions

RMSE: root mean square error

SAS: supercritical antisolvent precipitation

scCO$_2$: supercritical carbon dioxide

SCF: supercritical fluid

SCW: supercritical water

SFE: supercritical fluid extraction

SRK: Soave-Redlich-Kwong

VLE: vapor-liquid equilibrium

List of Symbols

a: Energy parameter [J·m^3/mol^2]

b: Co-volume parameter [m^3/mol]

i,j: counter

k: interaction parameter

T: temperature [K]

T_c: critical temperature [K]

T_r: reduced temperature [K]

P_c: critical pressure [MPa]

ω: acentric factor

V_m: molar volume [m^3/mol]

1. Introduction

The study of supercritical fluids is currently one of the lines of research with the greatest development, mainly due to the numerous industrial applications derived from them such as power generation, polymer processing or their use as an extracting agent in chemical processes and in the food industry. For this reason, experimental data sets, models, computer simulations and new measurement techniques are essential to be able to comprehensively understand the behaviour of these fluids and are necessary in the design of processes that use them. The fact that work is carried out at high pressure makes it even more important to know the properties of the mixtures used, not only in terms of performance but also in terms of safety.

In the present work, the high-pressure phase equilibrium study of a ternary system consisting of carbon dioxide, 2-propanol and 2-propanone is carried out by means of a synthetic measurement method, with the aim of extending the data set in high-pressure systems with carbon dioxide. So far, no system combining the three compounds has been found, although separate binary mixtures with carbon dioxide of the two organic solvents have been studied previously. It is therefore a novel system for which there is no previous literature with the same characteristics.

The importance of this study derives from the fact that, when a high weight proportion of carbon dioxide is applied at high pressure, it behaves as a poor to moderate solvent or as an anti-solvent that may be of interest in industrial processes. Isopropanol and acetone are compounds that can be involved in the same industrial process as in the production of acetone from isopropanol. Both organic solvents are widely used in the fine-chemical industry. With an eventual broadening of the use of supercritical fluids in fine-chemical production processes, readily available phase equilibrium data may be applied in process development. Also, their interest may lie, for example, in the fact that by applying these organic solvents along CO_2 in a low concentration ($\approx 5\%$), co-solvency effects could be achieved. They may also be used to dissolve target components prior to their antisolvent precipitation.

The paper describes the experimental process in which a high-pressure cell is used to observe the cloud points and redissolution points of the ternary mixture. It is applied for a temperature range between 35 and 55 ºC and the composition is varied between 0.70-0.99 CO_2 mole fraction to see the effect on the phase equilibrium at high pressure.

Subsequently, the results obtained from the experimentation are analysed using linear and quadratic response surfaces. This purely empirical analysis of the measured data can be used to determine the number of phases at a certain composition and temperature, or to calculate the minimum pressure (or maximum temperature) at which a homogeneous mixture can be formed, while setting the other parameter to a desired value. Thermodynamic modelling using the Peng-Robinson and Soave-Redlich-Kwong equations of state is carried out to determine binary interaction parameters between each component pair in the ternary system. The results may be used to more generally describe the behaviour of the mixture and to establish a basis for the future investigation of global phase equilibria.

2. Literature summary

2.1. Supercritical fluids: importance of phase equilibrium measurements

The use of supercritical fluids (SCFs) is currently one of the techniques with the largest research pipeline because they serve as a tool for the development of new and sustainable technologies. In recent years, further progress has been made in obtaining thermodynamic data that can be applied to these new technologies (Tsai and Wang 2019; Li and Xu 2019; Xu et al. 2021). The collection and analysis of these datasets is essential for the implementation of these techniques at the industrial level.

A supercritical fluid (SCF) is defined as one that has a temperature and pressure above the critical point (Figure 1), which gives it thermodynamic and fluid dynamic properties that are interesting for various industrial applications (Kiran and Sengers 1994). These fluids exhibit properties somewhere between a liquid and a gas, such as solvent behaviour or high diffusion respectively. Another characteristic of SCFs is the change in the behaviour of the density of the fluid by varying only the temperature or pressure without the appearance of an interface (Kiran et al. 2000). The viscosity in these fluids is much lower than that of the liquid. Near the critical point, slight changes in pressure and temperature lead to variations in important properties.
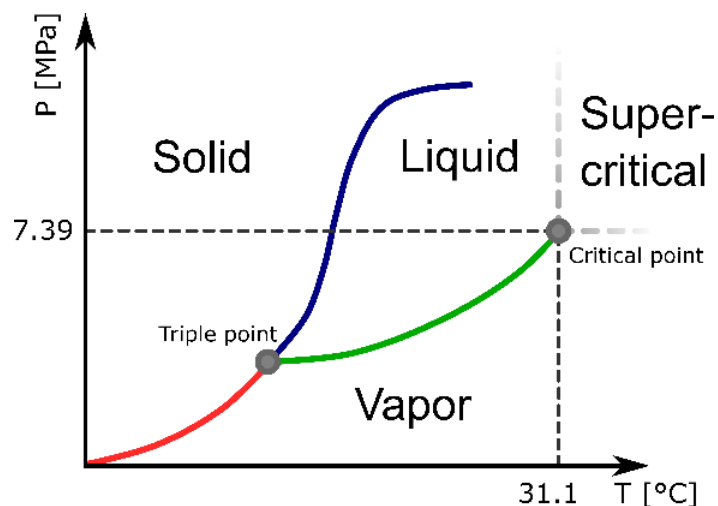
Figure 1. Single-component phase diagram with the critical pressure and temperature of carbon dioxide included.

The special properties and characteristics of these fluids mean that a thorough microscopic knowledge is necessary. SCFs react drastically to changes in certain

parameters, so it is important to be aware of this behaviour when mixtures are involved. These variations occur because those systems exhibit a wide range of fluctuations near the critical point, giving rise to anomalies in the vicinity of this point and making the thermodynamic behaviour and transport properties non-classical. These are long-range fluctuations in the order parameter related to the phase transition that are represented by the radius correlation (ξ) and which measure the degree of order across the boundaries of the phase transition system. As a result, small variations in pressure and temperature conditions represent large changes in the density and viscosity of the system (Nikolai et al. 2019).

The particularities associated with SCFs mean that the more information available, the better the understanding of the systems under study. In this sense, the development of dew-point and bubble-point curves is a fundamental field to predict the behaviour of the mixtures involved. In them, properties such as pressure and temperature are represented against the composition of some of the compounds of interest. The volatility of the solute used in the mixture determines the shape of the dew-point and bubble-point curves and they usually have a quadratic shape in relation to the solvent mole fraction. When the solution is dilute, the curves have a narrower shape and end in a peak shape at the critical point of the solvent. Figure 2 shows the dew-bubble-point isotherm curves in P-x, represented as a solid line. If the end of these curves is connected (dashed line), a tangent is obtained, the slope of which is given by the Krichevskii parameter (Kiran and Sengers 1994).
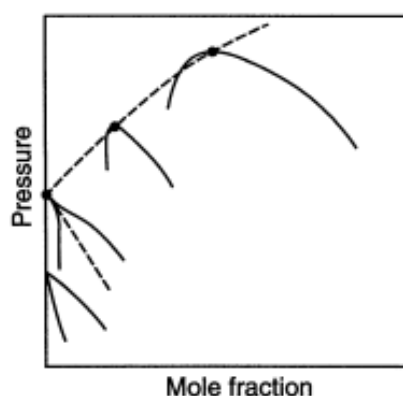
Figure 2. Dew-bubbles curves for a non-volatile solute at infinite dilution (Kiran and Sengers 1994).

The importance of obtaining a solid database has to do with the fact that parameters such as pressure and temperature are fundamental for the correct development of the processes in which the SCFs are involved. For instance, there are processes such as rapid expansion of supercritical solutions (RESS) where the compound of interest (e.g. a

polymer) is dissolved in the SCF at high pressure and depressurised through a nozzle to give rise to the precipitation phenomenon and the formation of a fine particulate product (Yeo and Kiran 2005). In the first part of the process, it is essential to set the right pressure and temperature to ensure that the compound to be precipitated is dissolved.

Gas antisolvent crystallization (GAS) is a batch process which is based on turning organic solutions of polar components oversaturated by mixing the solutions with pressurised carbon dioxide. The process is used to precipitate compounds that are not soluble in SCFs. The pressure and temperature must be set appropriately to ensure the extraction of the organic solvent with the supercritical fluid. If the filtered crystals can dissolve in the mixture, the phase equilibrium behaviour may change to a large extent as the effect of this minor component. It is therefore convenient to have measurements of the ternary system consisting of the organic solvent, SCF and solute (Yeo and Kiran 2005).

In supercritical antisolvent process (SAS) the compound of interest is dissolved in a solvent liquid and the solution is dispersed in a chamber where the SCF flows continuously. The contact between the two phases results in the supersaturation of the solution, leading to the creation of small particles due to rapid nucleation and growth (Yeo and Kiran 2005). Morphology or particle size distribution can be adjusted by changing the rate of depressurisation, the dissolved gas flow rate or the pressure and temperature that have previously been studied.

In supercritical fluid extraction (SFE), the target component must be soluble in SCF at the temperature and pressure of the extractor. However, in the separator, it must be able to precipitate, so, pressure is lowered below the minimum needed for dissolution at the temperature of the separator (Knez et al. 2013).

In aerogel drying, SCFs are also used, and pressure and temperature influence the drying time and other aspects like phase boundaries formation inside the pores of the gel. With supercritical carbon dioxide, phase boundary and surface tension within the gel are avoided. In this process, a homogeneous mixture of the organic solvent in which the gel is stable, and the CO_2 is first formed. Then, the organic solvent is extracted with supercritical CO_2 being present in the dryer. Finally, the pressure is reduced while maintaining above-critical temperature, which avoids the formation of a liquid-gas biphasic system and the collapse of the structure of the gel due to the strong surface tension (Shafi et al. 2021).

Historical examples where high-pressure equilibrium data collection has been important are the simulation of oil reservoirs, the transport and storage of natural gas or the study of geological processes, among others (Fonseca et al. 2011). However, technologies involving the use of SCFs are now presented among the most effective tools to satisfy the principles of Green Chemistry. This is a philosophy that aims to develop a model of ideal chemistry, where the developed compounds are as simple, environmentally friendly, safe, and effective in molecular terms as possible (Anastas and Eghbali 2010). Twelve principles govern this idea. The SCFs would be mainly related to the fifth principle, which talks about the use of safer solvents and auxiliaries being presented as a real alternative to traditional organic solvents. The carboxylic acid extraction with SCF over organic solvents is an example of this new trend, and although supercritical carbon dioxide extraction efficiencies are not as high as with 1-octanol, the use of a non-toxic and non-polluting solvent may be of interest from an environmental point of view (Djas and Henczka 2018). However, it must be considered that these processes often demand large amounts of energy due to the high pressure and temperature to which they must be subjected to overcome the critical point. Safety issues can be a challenge for the implementation of full-scale processes as well.

In line with this approach, some of the industrial applications for which these fluids are used have been compiled in recent years (Knez et al. 2014). Extraction of some substances such as essential oils, vitamins or pigments is possible with SCFs due to their good solubility in them. SCFs have also been used for the processing of particles as a solvent for monomers or anti-solvent for impregnation (Ramsey et al. 2009). Other uses of SCFs are cleaning or drying processes, for example, in the cleaning of oil-contaminated surfaces, as some SCFs such as carbon dioxide reduce the surface tension and viscosity, allowing the removal without leaving solvent residues. Also, it can be incorporated in sterilisation processes, very useful in the food industry or in medicine (Brunner 2010; Knez et al. 2014).

Many SCFs are of significant industrial interest. For example, there are studies using supercritical methanol (Han et al. 2020; Kong et al. 2021) or supercritical hydrocarbons with applications in the aeronautical industry (Xie et al. 2021). However, water and carbon dioxide are the most used SCF, mainly because they are more clearly linked to the concept of sustainability and are less expensive. For example, the use of supercritical water (SCW) is of particular interest for obtaining bioproducts and for waste treatment, as bio-oil, gases of interest as syngas or hydrogen, or biochar. These products can be

obtained directly from hydrothermal processes such as hydrothermal liquefaction (HTL), hydrothermal carbonization (HTC) or hydrothermal gasification (HTG) of biomass, among others (Knez et al. 2014). The advantage of some of these technologies is that they allow working with feedstocks with a high degree of moisture, avoiding the drying of the same at the entrance of the process, which results in significant energy savings. Despite this, it is necessary to assess the process from a global perspective due to the higher energy expenditure because of high pressure and temperature (Hrnčič et al. 2016).

Supercritical carbon dioxide ($scCO_2$) is probably the supercritical fluid with the widest variety of applications and articles available.

2.2.   Supercritical carbon dioxide ($scCO_2$)

There is a global trend towards the use of new sustainable and green technologies due to the growing need to eliminate more environmentally damaging processes and match increasingly restrictive regulations. In this context, $scCO_2$ has been presented as an alternative to other traditionally used compounds, such as organic solvents. What was more experimental work a few years ago is now becoming a reality at industrial level.

The market of products manufactured in processes with $scCO_2$ is a field that is constantly growing and the use of $scCO_2$ for energy purposes has led to an exponential increase in publications and patents in this field in recent years (Figure 3). Most of the patents associated with this topic have been developed in China (dark blue), while the literature has mainly been developed in other countries (White et al. 2021).
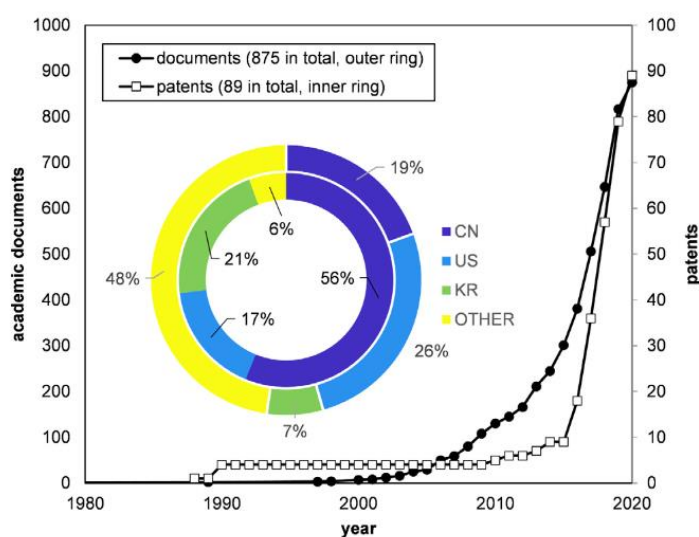
*Figure 3. Historical development and geographical distribution of publications and patents in the field of scCO2 power systems.*CN=People´s Republic of China; US= United States of America; KR=Republic of Korea; OTHER=Rest of the World (White et al. 2021).

14

The main advantage of scCO$_2$ has to do with its thermodynamic and transport properties that make it suitable for use in many industrial applications, which will be discussed in this section.

2.2.1. Properties and interest

ScCO$_2$ is non-toxic (in small quantities), non-flammable and can be considered relatively inert. It is also a compound that is available in large quantities and can be integrated into processes in a circular way in the future. Despite being a well-known greenhouse gas, if it is obtained from an environmentally benign source, these characteristics make it of particular interest as a green solvent, but it can also be used for the purpose of selectively dissolving a compound, among others (Boyère et al. 2014). Products of high added value may compensate for the costs of high-pressure industrial procedures.

The critical pressure (7.39 MPa) and critical temperature (31.1 ºC) of carbon dioxide, are relatively mild conditions to reach compared to other supercritical fluids such as water (Kiran et al. 2000). It is a poor solvent for polar substances, although some polar compounds such as acetone or methanol are soluble. Solubility increases for non-polar and low molecular weight substances (Boyère et al. 2014). On the other hand, it is a compound with a high diffusion rate, which results in supersaturated systems that allow the formation of particles with low particle size and a narrow particle size distribution (Wang et al. 2021).

This high capacity in transport and mass transfer properties coupled with a low viscosity make scCO$_2$ a fluid capable of replacing many organic solvents but also warns of good heat transfer, which makes it suitable for use in power generation processes (Crespi et al. 2017). In addition, other advantages that increase its interest for industrial applications are the feasibility of obtaining high purity carbon dioxide and its ability to be recovered and reintroduced into the process due to its high volatility (Nikolai et al. 2019). Another advantage is that carbon dioxide almost completely evaporates from the products. If said products are later ingested, the traces of carbon dioxide in them are not harmful, unlike those of many organic solvents, which may be of great interest for food applications.

2.2.2. Processes and applications.

The specific properties of scCO$_2$ result in several direct applications. Firstly, it can be used in solid-fluid extraction processes such as decaffeination of coffee and tea where the use of other conventional processes with higher temperatures is avoided (Wang et al. 2021) or the extraction of sesame oil (Brunner 2010). Selective extraction, purification and fractionation can be carried out easily by modifying the density of scCO$_2$. For instance, a low-density scCO$_2$ can imitate the polarity of n-pentane (non-polar) while a high-density scCO$_2$ can mimic the polarity of pyridine (polar) (Ramsey et al. 2009). The extraction of metals from aqueous solutions such as Cu^{2+}, Cr^{3+} or Zn^{2+} among others, is a direct application of the advantages of this compound as an extracting agent over organic solvents (Erkey 2000). Firstly, the volume of organic solvent used in conventional solvent extraction is usually high compared to scCO$_2$, as a specific organic solvent to aqueous phase ratio must be maintained. Secondly, the residual contamination of the aqueous phase is higher when organic solvents are used. Thirdly, the excellent diffusivity properties and low viscosities coupled with the low surface tension compared to organic solvents provides a larger contact area between the phases, resulting in a reduction of equipment size.

The second use has to do with the ability of this fluid to serve as a medium for different chemical reactions to take place. Frequently, reaction rates are enhanced and the energy required in the process is decreased compared to traditional solvents, due to the improved matter transfer of the fluid, leading to copolymerisation, oxidation, dimerization and trimerization, carbonylation and other reactions (Ramsey et al. 2009). At other times, however, reaction rates are lower, as in the Wacker reaction (Gang et al. 2003). Some authors have studied the characteristics of various polymerisation reactions in scCO$_2$ which are directly related to the synthesis of polymers, using techniques such as homogenisation, precipitation or for example dispersion polymerisation for the formation of PVC (poly(vinyl chloride)), PCL (polycaprolactone) or PDMS (poly(dimethyl siloxane) derivatives) among others (Boyère et al. 2014). In addition, scCO$_2$ can be used as a reaction medium and as a reactant at the same time, which has led to the study of improvements in the selectivity and yield of reactions in molecular catalysis (Ikariya and Kayaki 2000). Homogeneous and heterogeneous catalysis processes can be carried out in this medium (Ramsey et al. 2009) such as the hydroformylation process of olefins (Erkey 2011) or the hydrogenation of limonene (Bogel-Łukasik et al. 2010) respectively. The use

in biotechnological applications is also of great importance. Thus, enzyme stabilisation processes as well as reaction processes involving enzymes have been studied (Matsuda 2013). Polymer formation processes based on biocatalysis are also among the possibilities that are still being investigated (Ramsey et al. 2009).

Another application is the formation of aerogels by supercritical drying, where the original organic solvent in the gel is removed, giving rise to structures with a particular consistency, which can be used as catalyst supports or as drug carriers (Brunner 2010). Some of the factors in the preparation of aerogels from pure silica has recently been studied (Shafi et al. 2021).

Cleaning and degreasing procedures are other not so common processes where $scCO_2$ is used, replacing detergents, water, or organic solvents. This application, together with dyeing processes are starting to be applied in the textile industry, where the cost of wastewater treatment and the required water supply is known to be very high (Ramsey et al. 2009). The solubility of the dye needs to be known as a function of pressure and temperature, so it is important to know the phase equilibrium data. In addition, some natural fibres can be dyed without pre-treatment and the dyeing time can be greatly reduced with $scCO_2$ compared to other traditional disperse dyes (Brunner 2010). Supercritical carbon dioxide has also been utilized as a solvent in industrial-scale wood impregnation processes.

Finally, the use of $scCO_2$ as an agent in power generation cycles is again on the rise and it has been theoretically demonstrated that they can be competitive in the sense that they have a high versatility and high yields at moderate temperatures compared to other classical technologies (Crespi et al. 2017). Some of the potential markets for this technology are focused on industrial waste heat recovery, nuclear plants or bulk energy storage and geothermal $scCO_2$ power plants (Brun et al. 2017).

2.3.   Equilibrium measurement methods (modelling)

Phase equilibrium data to describe the behaviour of a system becomes valuable even during the early stage of the development of processes applying supercritical fluids. Precise laboratory measurement methodologies have been elaborated to efficiently gather the necessary information.

The methods used in these studies are mainly classified into two large families: analytical methods and synthetic methods (Figure 4). Both differ in whether the exact

composition of the equilibrium phases is determined, or the total composition of the mixture is known. Thus, analytical methods do not require knowledge of the total composition, but rather an analytical study of the coexisting phases is carried out (Fonseca et al. 2011).
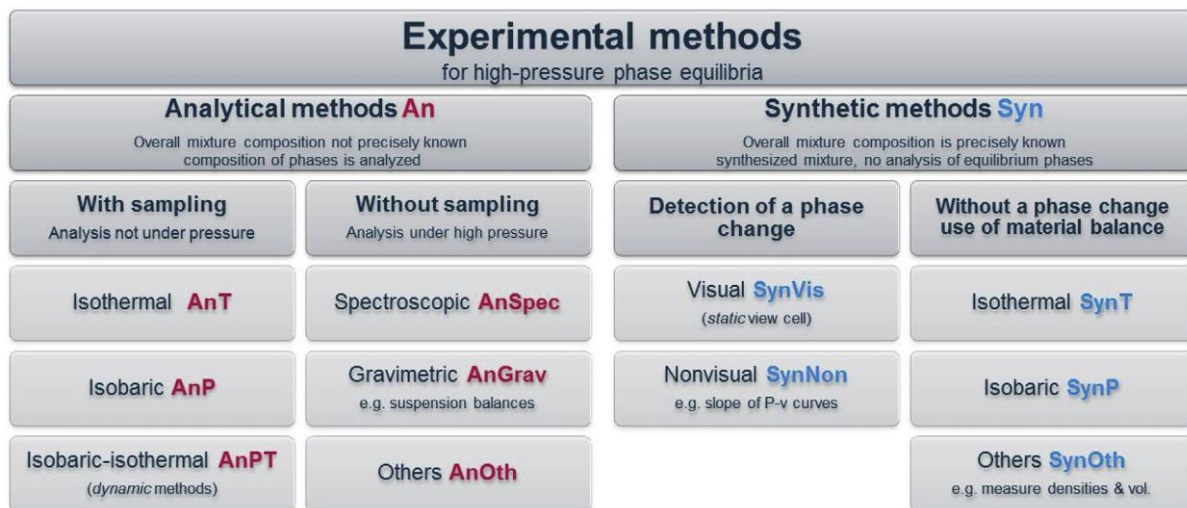
Figure 4. Classification of experimental methods for high-pressure phase equilibria (Peper et al. 2019).

These phases are subsequently analysed at atmospheric pressure by sampling (for example by chromatography) or without sampling and using physicochemical methods such as spectroscopy. Analytical methods with sampling include isothermal analytical methods (AnT), where the temperature stays constant during the process, isobaric analytical methods (AnP), where the pressure stays constant, or a combination of both (AnPT), where a stream is constantly pumped into a cell and the temperature is also controlled. Non-sampling methods include mainly spectrometric and gravimetric methods (Fonseca et al. 2011).

Synthetic methods are based on knowing the exact total composition of the mixture and then observing how it behaves at equilibrium without further sampling of the phase or phases. These methods differ in whether a phase transition occurs or not. In methods with phase transition, first the pressure and temperature conditions of the system must be adjusted to obtain a single homogeneous phase. Subsequently, the pressure or temperature is varied until there is an abrupt change in the system indicating the formation (or disappearance) of a new phase the composition of which is not known. Depending on whether the phase transition is detected visually or not, the methods can be divided into visual (SynVis) or non-visual (SynNon) groups. Figure 5 shows a visual synthetic process in which the different phase equilibria can be observed (Braga et al. 2021). Picture 1 shows a completely homogeneous system where only one liquid phase is visible. Picture

2 shows a system with two liquid phases while picture 3 shows a vapour phase and two liquid phases. The white object at the bottom is a magnetic stirrer.
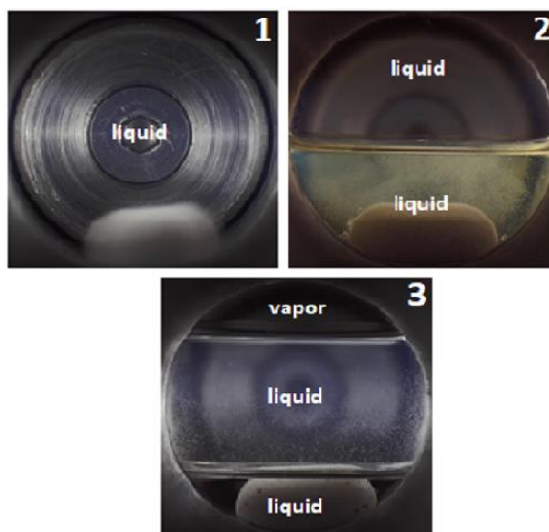
Figure 5. Image of phase transitions for the system CO_2 + n-hexadecane like those observed in this work (Braga et al. 2021).

In non-phase transition methods, the mass balance is used to calculate the compositions and other properties such as temperature, pressure, volumes of each phase or densities are measured. There are isothermal (SynT), isobaric (SynP), or other methods (SynOth). In the isothermal process, a compound with exactly known amount is introduced into the cell before it is brought to the temperature that is set. Subsequently, a known exact amount of a second compound is introduced into the cell and a pressure drop occurs after dissolving in the liquid phase. The composition of the vapour phase can be calculated from phase equilibrium models using pressure and temperature measured in the cell. The mass and component balance is used to calculate the liquid's composition. The process would be similar for the isobaric method but setting a constant pressure. Synthetic methods are often used to solve problems that may arise when using analytical methods, such as in systems where there is no good phase separation due to the very similar densities of the forming phases. In addition, they are faster methods as they avoid the characterisation of the samples (Fonseca et al. 2011; Peper et al. 2019)

In obtaining thermodynamic data, it is desirable that systems are studied by a larger number of authors and therefore, combining the use of synthetic and analytical methods as well as the use of different equipment. In this way, the validation of the results can be carried out and the new data set is contrasted. This work uses a synthetic method with visual phase transition in a static cell.

2.4. Short review on the ternary mixtures available

There are many pure substances that can be combined and that can give rise to different phase equilibrium situations. Such situations may include the mixture of carbon dioxide and a single co-solvent, eventually in the presence of a solute (forming a ternary mixture). In case of multiple co-solvents to tune the polarity and dissolving capability of the mixture, even more complex phase behaviour may be expected. In each process, where a mixture is applied, the phase behaviour has to be taken into account, whether there will be one homogeneous phase or multiple phases under the circumstances to be established, and the behaviour of the system has to be carefully analysed. This work focuses mainly on the use of three compounds, namely 2-propanol (isopropanol), 2-propanone (acetone) and carbon dioxide.

Acetone and isopropanol are common chemical compounds the behaviour of which has been studied. There is a large body of literature in which these compounds are used separately (Pasanen et al. 2006; Lazzaroni et al. 2006; Wang et al. 2021), although their occurrence together in ternary systems is non-existing. The importance of this work lies in the fact that it has studied a system that has not been previously analysed. It should be noted that this work focuses on high-pressure systems, traditionally considered to be those where the pressure is above 1 MPa. For isopropanol, there are different studies working with the pure compound, in varying temperature ranges, from which the critical parameters of the compound can be obtained (Dell'Era et al. 2007; Khoiroh and Lee 2011; Keshtkari et al. 2013). Authors of other papers have studied different thermodynamic properties of pure acetone between 5-50 °C and at high pressures (Malhotra and Woolf 1991). The breadth of literature on systems studying carbon dioxide is greater, mainly due to the possible applications described above in high-pressure systems. Generally, these publications deal with the study of the equilibrium of binary mixtures, but the behaviour of pure carbon dioxide is also studied in a temperature range similar to the present work (Kim et al. 2010; Fonseca and von Solms 2012). There are also studies where these compounds are combined as part of binary, ternary or quaternary mixtures where the pressure ranges are varied and may include carbon dioxide (Peper et al. 2019).

For instance, the CO_2-acetone binary system is a mixture that has been studied in detail. Some studies use an isochoric technique to investigate its behaviour and to obtain the dew points in areas close to the critical region (pressure and temperature) (Wu et al. 2004). There are others that also study this system, focusing on solubility of CO_2 in

acetone and 1-butyl-3-methylimidazolium tetrafluoroborate (Lei et al. 2012) or using a continuous process that takes advantage of the change in signal from a Flame Ionisation Detector (FID) (Novitskiy et al. 2009). Some studies related to volumetric expansion in binary CO_2 systems with some ketones, such as acetone, cite the presence of a slow volume expansion zone up to a CO_2 mole fraction of 0.7 and a fast volume expansion zone above this value (Aida et al. 2010). Another study correlates the experimental results using the Peng-Robinson equation of state and the generalised version of the Bender equation of state (Bamberger and Maurer 2000).

Studies of binary mixtures of carbon dioxide with isopropanol are not as numerous as for acetone but they are common and have been studied since the last quarter of the 20th century (Radosz 1986; Suzuki et al. 1991; Yaginuma et al. 1997). The presence of a cell for equilibrium measurements is already common at this time and properties such as solubility or density are studied. Also, there are studies using the binary mixture of carbon dioxide with isopropanol to validate a new method or to jointly determine vapour-liquid equilibrium (VLE) data and saturation densities (Galicia-Luna and Elizalde-Solis 2010).

There are also articles where acetone and isopropanol appear together in the same study with carbon dioxide, either separately (Bamberger and Maurer 2000) or as part of ternary or quaternary systems together with other compounds such as argon (Lazzaroni et al. 2006). Some ternary systems formed by water + fluoromethane + isopropanol/acetone have been studied due to their importance in hydrate formation processes (Imai et al. 2012). The effect of salting out has also been studied in multiphase systems consisting of ethene, water and isopropanol to which an electrolyte is added. The aim of these experiments is to analyse this effect in systems using biomolecules to be extracted or to avoid their denaturation by adjusting the pH or the ionic strength of the solution (Ulanova et al. 2009). As for studies of ternary mixtures involving carbon dioxide together with acetone/isopropanol and a third compound, the present literature is abundant. For isopropanol, the number of studies is smaller than for acetone. Some examples are the use of synthetic methods with isopropanol as co-solvent in mixtures with palmitic acid (Brandt et al. 2010) or the study of phase behaviour when mixed with an ionic liquid such as 1-hexyl-3-methylimidazolium tetrafluoroborate (Kroon et al. 2010). For acetone, the variety of compounds used is greater. For example, the study of the structures of the hydrates formed with the use of supercritical CO_2 and their stability were studied for different mole fractions of acetone (Maekawa 2011). As with isopropanol, studies have also been carried out with ionic liquids such as 1-butyl-3-

21

methylimidazolium tetrafluoroborate (Lei et al. 2012). Studies on these systems typically cover temperature ranges of around 50 °C (Peper et al. 2019), however, there are some more specific reviews carried out at much higher temperatures (>150 ºC) working with compounds such as β-cyclodextrin (Grandelli et al. 2012). Table 1 summarises the literature of relevance to this work.

Table 1. Summary of literature on high-pressure studies with the compounds involved in this work.

Mixture	Conditions of the study	Modelling
CO_2 (i)+acetone(j) *(Wu et al. 2004)*	T(K): 313.2 and 393.2 P(MPa): 4.19-43.06 CO_2 mole fraction: 0.9	Correlation with Peng-Robinson (PR) EOS and Sánchez-Lacomb (SL) EOS. PR mixing rule. PR k_{ij} = -0.03
(Lei et al. 2012)	T(K): 298.2; 313.2 and 323.2 P(MPa): > 6 CO_2 mole fraction: 0.1-0.9	PR EOS and PR mixing rule. k_{ij} non-temperature dependant between 298.2 and 323.2. PR k_{ij}= 0.007
(Novitskiy et al. 2009)	T(K): 350-380 P(MPa): 7.3-11.6 CO_2 mole fraction: 0.2 and 0.7	Does not model the data
(Bamberger and Maurer 2000)	T(K): 293-333 P(MPa): 7.3-11.6 CO_2 mole fraction: 0-1	PR EOS modified with Melhem and Generalized Bender EOS. Mixing rules of Panagiotopoulos and Reid. PR k_{ij}= -0.0251; k_{ji}= -0.0008
CO_2 (i)+ isopropanol (j) *(Radosz 1986)*	T(K): 317;335;354 and 394 P(MPa): 1.4-12 CO_2 mole fraction: 0.45-0.60	Soave-Redlich-Kwong (SRK), PR and Zudkevitch and Joffe (RKJZ) EOS. Van der Waals on-fluid mixing rules. SRK k_{ij}= 0.098; PR k_{ij}= 0.107
(Suzuki et al. 1991)	T(K): 313.7 and 333.7 P(MPa): >11 CO_2 mole fraction: 0.95-1	No correlation. Enhancement factor method for solubility consistency.
(Yaginuma et al. 1997)	T(K): 313.5 P(MPa): >9.8 CO_2 mol fraction: 0-1	No correlation. VLE and density curves.
(Galicia-Luna and Elizalde-Solis 2010)	T(K): 313-363 P(MPa): 2.4-12.5 CO_2 mole fraction: 0.1-0.9	Peng–Robinson equation of state coupled to classical and Wong–Sandler mixing rules. PR 0.111≤k_{ij}≤0,128 (T-dep.)
(Bamberger and Maurer 2000)	T(K): 293-333 P(MPa): 7.3-11.6 CO_2 mol fraction: 0-1	PR EOS modified with Melhem and Generalized Bender EOS. Mixing rules of Panagiotopoulos and Reid. PR k_{ij}= 0.1467; k_{ji}= 0.1005
Others *(Lazzaroni et al. 2006)* CO_2 + isopr.+ argon (1) CO_2 + isopr. + argon + acetone (2)	T(K): 313 P(MPa): 6.9-15 CO_2 mol fraction (1): 0.15-0.85 CO_2 mol fraction (2): 0.27-0.48	Patel-Teja (PT) EOS. Mathias–Klotz–Prausnitz (MKP) mixing rules. k_{ij}: temperature dependant
(Brandt et al. 2010) CO_2 + palmitic acid + isopr.	Tª(K): 313-318 P(MPa): 10-25 CO_2 mol fraction (2): 0.94 and 0.97	Density-based models proposed by Mendez-Santiago and Teja for consistency of the data

3. Materials and methods

3.1. Materials

The three compounds used are carbon dioxide, 2-propanone (acetone) and 2-propanol (isopropanol). The carbon dioxide was supplied by Linde Gas Hungary. The purity of this carbon dioxide (product Biogon C for food industry applications) is approximately 95 %. Carbon dioxide is used in all of the laboratory equipment freshly distilled. The acetone was supplied by Carlo Erba and had a purity of over 99.8% (GC) and isopropanol was supplied by Merck with a purity of over 99.5% (GC). The properties of the compounds are summarised in Table 2.

Table 2. Compounds used in this work.

Chemical Name	CAS Number	Source	Purity (% mol)
2-propanone	67-64-1	Carlo Erba	99.8
2-propanol	67-63-0	Merck	99.5
Carbon dioxide	124-38-9	Linde Gas Hungary	95

3.2. Experimental method

The main objective of the measurements carried out is to obtain a set of data that can be applied over a range of temperatures and compositions for the ternary equilibrium of carbon dioxide, 2-propanone (acetone) and 2-propanol (isopropanol). Acetone and isopropanol may be used as organic solvents in for example antisolvent fractionation.

The measurements were carried out in a high-pressure view-cell (New Ways of Analytics GmbH.) containing two sapphire windows that allow the interior to be illuminated and fully visible from the outside (Figure 6). The cell can be used at a maximum pressure of 60 MPa and a maximum temperature of 250 °C. The illumination is carried out with a high brightness LED. The view of the cylindrical cell is provided horizontally. The cell is assembled using a circular set of screws between the lid and the rest of the cell. The sample to be tested can be introduced by removing this cover or through the opening corresponding to the temperature sensor. The choice depends on the state of the sample, in this case, liquid mixtures are used, so the sample is introduced through the ¼" opening of the temperature sensor (1.) by means of a measuring pipette.

The exact quantity of the components of the organic solvent mixture was determined by weighing on an analytical balance in each measurement.
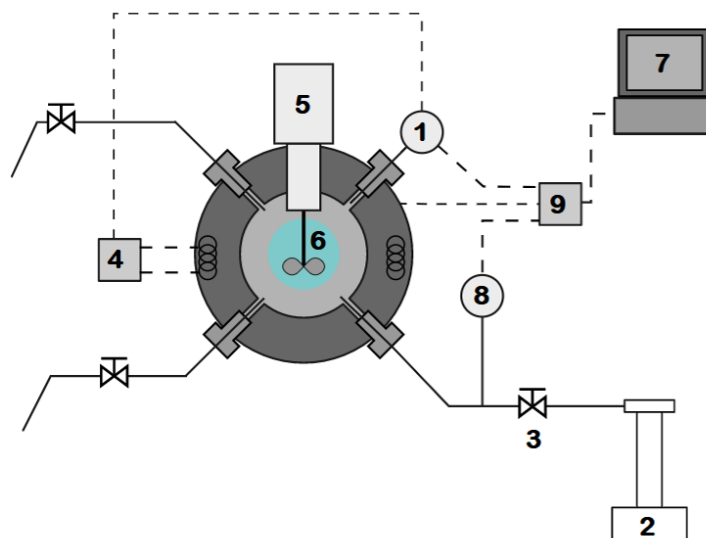
Figure 6. Schematic representation of the cell (Kőrösi et al. 2019).

(1.) Temperature sensor; (2.) Teledyene ISCO 260D syringe pump; (3.) Control valve; (4.) Temperature controller; (5.) Stirrer; (6.) Piston and viewing area of the cell; (7.) Computer; (8.) Pressure transducer; (9.) Analog-Digital converter and amplifier.

The Teledyne ISCO 260D syringe pump (2.) is used to pressurise the cell and allows to determine the amount of CO_2 introduced into the unit. The volumetric flowrate can be regulated by means of a control valve (3.). The pump maintains constant pressure in its cylinder by automatically actuating its piston. The cylinder is tempered, and its momentary volume is displayed by the pump. The temperature of the circulated water in the jacket is measured and is used to approximate that of carbon dioxide inside the cylinder. The amount of carbon dioxide filled into the cell can be determined based on the change in the stored volume inside the pump. The temperature of the cell can be easily regulated with two heating rods that are inserted into the wall of the cell and which are controlled by a temperature controller (4.). The unit also has a thermostatic jacket through which a cooling fluid can circulate. The solution inside is stirred by magnetically coupled turbine mixer the speed of which can be controlled by a speed controller (5.). In this case, the speed is not specified, but it is sufficient to ensure the correct homogeneous mixing. At the back of the cell, a piston regulates the volume of the cell which can be modified during high-pressure measurements (6.), allowing the change in pressure without changing the temperature and vice versa. The cell volume can be changed with this piston between a minimum of approximately 39 mL and a maximum value of 70 mL. One of

the issues reported in reviews of equilibrium data collection is that around 50% of the data reported between 1988 and 2012 used cells of this type with volumes between 10 and 100 mL, although smaller and smaller volumes are increasingly being used (Peper et al. 2019).

 Cell pressure, temperature and volume are recorded in a computer (7.). Opacity and redissolution points can be recorded in the data. For this purpose, the cell is equipped with a mobile control that allows the user to press a key and instantly display these points on the screen. A pressure transducer (8.) and an analogue-digital converter and amplifier (9.) are also present in the installation.

The method applied in this work is the visual static-synthetic method where a previous preparation of the samples is carried out. When the overall composition is known, the phase envelope can be traced without requiring a sampling process and reducing the complexity of the experimental method. A series of mixtures of 2-propanone and 2-propanol were prepared based on their volumetric ratio (Table 3). The exact amount was determined based on the mass of the solvents.

Table 3. Measurements conducted in this work.

Volumetric ratio acetone/isopropanol	Quantity fed into reactor (mL)	Temperature range studied
1:1		
3:1	0.25 /1/ 3 /5 /15	35 ℃-55 ℃ (ΔT 5 ℃)
5:1		

The pressure at which CO_2 is charged through the syringe pump is 20 MPa and the CO_2 is at a temperature of around 25 ℃. This temperature is measured in each experiment to ensure a correct calculation of the global composition introduced into the cell through density. The density of carbon dioxide was obtained using the database of NIST (NIST 2021). The temperature range for which data is taken is 35 to 55 ℃ with a temperature increase of 5 ℃ for each measurement.

A typical experiment consists of introducing the sample into the cell. Subsequently, the cell is sealed, and pressurisation of the cell begins once there is equilibrium in the channels between the syringe pump and the cell itself (the volumetric flowrate displayed by the pump falls below 0.1 mL/min). When this state is reached, CO_2 is introduced into the cell and the pressure starts to increase and tempering is also initiated. This process is carried out at maximum volume, until a sufficient pressure is reached in the equipment

(e.g. 3 MPa). At this point, the piston can be activated to bring the cell to a minimum volume (~ 39 mL). When not in use, the cell is stored at maximum volume. As a pneumatic system is used to actuate its piston, it is usually not operated with the cell being at ambient pressure to avoid too quick movements of the piston. Pressurisation continues until the mixture inside is homogeneous. This homogenisation takes place in the experiment at around 8 MPa. From this point on, the experimental process is based solely on the modification of the volume by means of the piston. The increase in volume (accompanied by a decrease in pressure) results in the opacity of the sample solution. The reduction of the volume leads to the redissolution of the sample.

The measurement process is robust and can be carried out routinely to obtain significant amounts of phase equilibrium data. The person taking the measurement observes the inside of the cell visually. For this purpose, the glass should be completely clean. One must be alert to the abrupt change in the system to activate a control that marks the point of opacity or redissolution, and this is recorded in the computer. As mentioned above, this process was conducted for organic solvent volumes of 0.25, 1,3, 5 and 15 mL loaded into the view-cell. In this way, a varied range of compositions is established. However, after covering the planned temperature range in the experiment, an amount of carbon dioxide of about 5 mL (at the parameters of the ISCO pump) was added to increase this range of compositions. This addition in the laboratory is done with the ISCO pump, again by measuring the temperature of the carbon dioxide introduced.

The reliability of the data collected is shown to be one of the most important facts in the study. For each mole fraction and temperature, at least three measurements of the opacity and redissolution points were taken. Most commonly, four data were taken and those values with anomalies (for example significantly different temperatures compared to the intended value) were discarded, although sometimes up to five measurements were taken. The raw measurement data is presented in Appendix 7.2 and 7.3. For the opacity point, where the visualisation is clearer, anomalies were those that differ by approximately 5 % in relative pressure terms. For the redissolution point, with a lower clarity of measurements, this range was extended to about 10 %.

Visually, what is seen in the cell is a single phase that becomes distinctly cloudy when it reaches the point of opacity. Conversely, the opacity ends at the redissolution point, where the solution becomes clear again. A similar idea to the one applied here can be seen in *Braga et al. 2021*, where the phase transitions are visually observed in a new type of cell very similar to the one studied here. One of the main problems in data collection is

the difficulty in clearly observing opacity or redissolution in the cell. This usually occurs when the mole fraction of carbon dioxide increases or when the temperature is higher. When this happens, rather than a visual change in the dissolution, a certain pumping can sometimes be seen, which is associated with these points.

3.3. Calculation methods.

This chapter presents the essential calculations that are carried out in the work. The amount of carbon dioxide added in the cell is calculated from the molar difference measured in the laboratory at the ISCO pump. As the pump displays the momentary volume of its cylinder, the molar density of the carbon dioxide was needed to obtain molar values. The values of this molar density are obtained from the NIST database (NIST 2021) at a pressure of 200 bar.

$$\Delta n_{CO_2} = n_{initial;ISCO} - n_{final;ISCO} \qquad [\,1.]$$

Where:

Δn_{CO_2}: moles of CO_2 introduced into the cell

$n_{initial;ISCO}$: initial amount of CO_2 in the ISCO pump (mol)

$n_{final;ISCO}$: final amount of CO_2 in the ISCO pump (mol)

For the calculation of the initial and final quantity of carbon dioxide in the cylinder:

$$n_i = \rho_{n;CO_2} \cdot V_{i;ISCO} \qquad [\,2.]$$

Where:

n: mol of CO_2 in the initial and final situation of the ISCO pump, the states are differentiated by the subscript i (mol)

$\rho_{n;CO_2}$: molar density of CO_2 at the corresponding temperature and pressure (mol/mL)

$V_{i;ISCO}$: initial or final volume of CO_2 in the ISCO pump, the states are differentiated by the subscript i (mL)

The molar quantity of each organic solvent (specified by the subscript j) was calculated from the molecular weights of acetone and isopropanol (MW_acetone: 58.08 g/mol ; MW_isopropanol: 60.09 g/mol)

$$n_j = \frac{m_j}{MW_j} \qquad \textit{[3.]}$$

Where:

n_j: moles of organic solvent j

m_j: mass of organic solvent j (g)

MW_j: molar weight of organic solvent j (g/mol)

The mole fraction for each compound is expressed as follows for organic solvents:

$$x_j = \frac{n_j}{n_{total}} \qquad \textit{[4.]}$$

Where:

n_{total}: sum of the moles of the organic solvents and CO_2.

And in the same way for CO_2:

$$x_{CO_2} = \frac{n_{CO_2}}{n_{total}} \qquad \textit{[5.]}$$

It is essential to check that the sum of all mole fractions is equal to 1:

$$\sum_j x + x_{CO_2} = 1 \qquad \textit{[6.]}$$

When extra CO_2 is added, the mole fractions of the mixture must be recalculated. The number of moles of organics remains unchanged, however, the moles of CO_2 increase:

$$n_{new_{CO2}} = n_{CO_2} + n_{extra} \qquad \textit{[7.]}$$

The procedure for the calculation of the extra moles of CO_2 is the same as in *[1.]*, *[2.]* and *[3.]*. The mole fractions must be recalculated in the same way, as the total number of moles also changes.

28

4. Results

The main results obtained are explained below. First, an analysis of the raw data is carried out. The response-surfaces constructed to fit the data lack a thermodynamic background. However, they can be easily used in further laboratory experiments carried out in the already investigated composition and temperature ranges to relatively accurately predict the pressure at which a homogeneous mixture may be expected. Subsequently, the results are discussed from the perspective of thermodynamic analysis. The computational analysis of the data in a process simulation software, using widely applied equations of state is more generally useful. While it falls back in prediction accuracy compared to the purely empirical response-surface technique, its results may later become applied in global phase equilibrium studies as well as used by a wider community of researchers.

4.1. Measured data

The study demonstrates that data collection requires many measurements to obtain a representative data set. The experimentation consists of about 1030 individual measurement points since for each temperature and composition setting at least 3 measurements are taken. The average opacity and redissolution data are summarised in Table 4 and Table 5, respectively.

Table 4. Average data of the opacity points for each composition (1/5).

Volumetric ratio of organic solvents	x_{CO2}	$x_{acetone}$	$x_{isopropanol}$	T [K]	P[MPa]
	0.7118	0.1476	0.1406	306.75	5.32
	0.7118	0.1476	0.1406	312.12	5.71
	0.7118	0.1476	0.1406	317.28	5.99
	0.7118	0.1476	0.1406	322.42	6.90
	0.7118	0.1476	0.1406	326.32	7.14
	0.7491	0.1285	0.1224	307.43	5.70
1:1 Acet/Isopr	0.7491	0.1285	0.1224	311.30	5.92
	0.7491	0.1285	0.1224	316.83	6.71
	0.7491	0.1285	0.1224	321.63	6.96
	0.7491	0.1285	0.1224	327.75	7.59
	0.8930	0.0540	0.0530	307.85	6.89
	0.8930	0.0540	0.0530	312.75	7.50

29

Volumetric ratio of organic solvents	x_{CO2}	$x_{acetone}$	$x_{isopropanol}$	T [K]	P[MPa]
	0.8930	0.0540	0.0530	317.55	7.97
	0.8930	0.0540	0.0530	322.82	9.07
	0.8930	0.0540	0.0530	327.28	9.65
	0.9351	0.0326	0.0323	307.98	7.15
	0.9351	0.0326	0.0323	312.35	7.87
	0.9351	0.0326	0.0323	317.08	8.37
	0.9351	0.0326	0.0323	322.45	8.89
	0.9351	0.0326	0.0323	327.82	9.75
	0.9444	0.0280	0.0277	307.28	7.23
	0.9444	0.0280	0.0277	311.65	7.62
	0.9444	0.0280	0.0277	318.12	8.56
	0.9444	0.0280	0.0277	322.78	9.06
	0.9444	0.0280	0.0277	327.98	9.51
	0.9798	0.0103	0.0099	307.08	7.17
	0.9798	0.0103	0.0099	311.80	7.67
1:1 Acet/Isopr	0.9798	0.0103	0.0099	317.18	8.30
	0.9798	0.0103	0.0099	322.30	8.86
	0.9798	0.0103	0.0099	327.63	9.51
	0.9822	0.0091	0.0087	307.38	7.20
	0.9822	0.0091	0.0087	312.43	7.65
	0.9822	0.0091	0.0087	317.68	8.27
	0.9822	0.0091	0.0087	322.60	8.96
	0.9822	0.0091	0.0087	327.75	9.84
	0.9939	0.0031	0.0030	306.45	7.13
	0.9939	0.0031	0.0030	311.95	7.49
	0.9939	0.0031	0.0030	317.30	8.19
	0.9939	0.0031	0.0030	322.50	8.69
	0.9939	0.0031	0.0030	327.08	9.36
	0.9948	0.0026	0.0025	306.40	7.16
	0.9948	0.0026	0.0025	312.28	7.64
	0.9948	0.0026	0.0025	317.53	8.12
	0.9948	0.0026	0.0025	321.98	8.77
	0.9948	0.0026	0.0025	327.83	9.47
	0.7668	0.1750	0.0582	307.60	5.65
3:1 Acet/Isopr	0.7668	0.1750	0.0582	312.15	6.00

Volumetric ratio of organic solvents	x_{CO2}	$x_{acetone}$	$x_{isopropanol}$	T [K]	P[MPa]
	0.7668	0.1750	0.0582	316.23	6.91
	0.7668	0.1750	0.0582	321.50	6.94
	0.7668	0.1750	0.0582	327.15	7.77
	0.7927	0.1556	0.0518	309.03	5.82
	0.7927	0.1556	0.0518	311.98	6.79
	0.7927	0.1556	0.0518	317.13	7.03
	0.7927	0.1556	0.0518	320.63	7.24
	0.7927	0.1556	0.0518	328.80	7.99
	0.9052	0.0711	0.0237	306.93	6.76
	0.9052	0.0711	0.0237	312.55	7.23
	0.9052	0.0711	0.0237	317.85	7.83
	0.9052	0.0711	0.0237	322.22	8.49
	0.9052	0.0711	0.0237	327.58	9.22
	0.9181	0.0614	0.0204	307.28	6.77
	0.9181	0.0614	0.0204	311.55	7.35
3:1 Acet/Isopr	0.9181	0.0614	0.0204	317.85	8.08
	0.9181	0.0614	0.0204	323.38	8.94
	0.9181	0.0614	0.0204	327.08	10.37
	0.9512	0.0366	0.0122	307.60	7.25
	0.9512	0.0366	0.0122	311.58	7.73
	0.9512	0.0366	0.0122	315.98	8.38
	0.9512	0.0366	0.0122	321.43	9.25
	0.9512	0.0366	0.0122	327.83	10.05
	0.9570	0.0323	0.0107	307.35	7.38
	0.9570	0.0323	0.0107	311.03	7.80
	0.9570	0.0323	0.0107	316.03	8.48
	0.9570	0.0323	0.0107	320.55	9.47
	0.9570	0.0323	0.0107	326.05	10.21
	0.9775	0.0169	0.0056	308.40	7.21
	0.9775	0.0169	0.0056	312.63	7.84
	0.9775	0.0169	0.0056	316.55	8.25
	0.9775	0.0169	0.0056	322.13	9.52
	0.9775	0.0169	0.0056	327.83	11.32
	0.9810	0.0143	0.0047	307.75	7.46
	0.9810	0.0143	0.0047	312.93	8.06
	0.9810	0.0143	0.0047	317.13	8.55

31

Volumetric ratio of organic solvents	x_{CO2}	$x_{acetone}$	$x_{isopropanol}$	T [K]	P[MPa]
	0.9810	0.0143	0.0047	322.58	10.06
	0.9810	0.0143	0.0047	327.73	11.54
	0.9988	0.0009	0.0003	307.18	7.21
3:1 Acet/Isopr	0.9988	0.0009	0.0003	312.08	7.57
	0.9988	0.0009	0.0003	317.08	8.20
	0.9988	0.0009	0.0003	322.58	8.87
	0.9988	0.0009	0.0003	327.03	9.55
	0.7129	0.2401	0.0471	307.95	5.03
	0.7129	0.2401	0.0471	312.45	5.71
	0.7129	0.2401	0.0471	317.65	5.90
	0.7129	0.2401	0.0471	322.48	6.26
	0.7129	0.2401	0.0471	326.62	7.06
	0.7499	0.2091	0.0410	307.52	5.30
	0.7499	0.2091	0.0410	310.78	6.00
	0.7499	0.2091	0.0410	313.52	6.41
	0.7499	0.2091	0.0410	323.32	6.93
	0.7499	0.2091	0.0410	327.48	7.35
	0.8961	0.0877	0.0162	307.45	6.55
	0.8961	0.0877	0.0162	312.62	7.25
5:1 Acet/Isopr	0.8961	0.0877	0.0162	316.35	7.98
	0.8961	0.0877	0.0162	322.48	8.88
	0.8961	0.0877	0.0162	327.30	9.35
	0.9100	0.0760	0.0140	307.88	6.71
	0.9100	0.0760	0.0140	313.05	7.50
	0.9100	0.0760	0.0140	317.02	7.98
	0.9100	0.0760	0.0140	322.65	8.67
	0.9100	0.0760	0.0140	327.55	9.71
	0.9368	0.0534	0.0098	307.35	7.01
	0.9368	0.0534	0.0098	312.00	7.70
	0.9368	0.0534	0.0098	317.53	8.19
	0.9368	0.0534	0.0098	322.63	9.16
	0.9368	0.0534	0.0098	327.15	10.40
	0.9454	0.0461	0.0085	306.95	7.11
	0.9454	0.0461	0.0085	311.45	7.59
	0.9454	0.0461	0.0085	317.28	8.57
	0.9454	0.0461	0.0085	321.75	9.09

Table 4. Average data of the opacity points for each composition (5/5).

Volumetric ratio of organic solvents	x_{CO2}	$x_{acetone}$	$x_{isopropanol}$	T [K]	P[MPa]
	0.9454	0.0461	0.0085	327.68	10.23
	0.9759	0.0203	0.0037	307.40	7.32
	0.9759	0.0203	0.0037	311.90	7.80
	0.9759	0.0203	0.0037	316.85	8.50
	0.9759	0.0203	0.0037	322.63	9.56
	0.9759	0.0203	0.0037	327.40	10.38
	0.9796	0.0172	0.0032	307.43	7.29
	0.9796	0.0172	0.0032	311.83	8.03
5:1 Acet/Isopr.	0.9796	0.0172	0.0032	318.13	9.03
	0.9796	0.0172	0.0032	321.98	10.02
	0.9796	0.0172	0.0032	327.25	10.93
	0.9938	0.0050	0.0011	310.08	7.45
	0.9938	0.0050	0.0011	314.40	8.14
	0.9938	0.0050	0.0011	318.38	8.61
	0.9938	0.0050	0.0011	323.55	9.04
	0.9938	0.0050	0.0011	328.60	9.62

Table 5. Average data of the redissolution points for each composition (1/5).

Volumetric ratio of organic solvents	x_{CO2}	$x_{acetone}$	$x_{isopropanol}$	T [K]	P[MPa]
	0.7118	0.1476	0.1406	308.45	5.85
	0.7118	0.1476	0.1406	313.98	6.33
	0.7118	0.1476	0.1406	319.58	6.96
	0.7118	0.1476	0.1406	324.62	7.68
	0.7118	0.1476	0.1406	327.48	7.89
	0.7491	0.1285	0.1224	311.63	6.77
	0.7491	0.1285	0.1224	314.58	6.59
1:1 Acet/Isopr.	0.7491	0.1285	0.1224	319.60	7.28
	0.7491	0.1285	0.1224	323.65	7.55
	0.7491	0.1285	0.1224	329.03	7.95
	0.8930	0.0540	0.0530	310.05	7.23
	0.8930	0.0540	0.0530	315.35	7.65
	0.8930	0.0540	0.0530	318.85	8.03
	0.8930	0.0540	0.0530	325.68	9.90
	0.8930	0.0540	0.0530	329.82	10.64
	0.9351	0.0326	0.0323	310.55	8.15

Table 5. Average data of the redissolution points for each composition (2/5).

Volumetric ratio of organic solvents	x_{CO2}	$x_{acetone}$	$x_{isopropanol}$	T [K]	P [MPa]
	0.9351	0.0326	0.0323	314.52	8.41
	0.9351	0.0326	0.0323	319.05	9.23
	0.9351	0.0326	0.0323	324.18	9.45
	0.9351	0.0326	0.0323	330.12	10.03
	0.9444	0.0280	0.0277	309.35	8.15
	0.9444	0.0280	0.0277	313.95	8.45
	0.9444	0.0280	0.0277	319.08	8.70
	0.9444	0.0280	0.0277	325.25	9.76
	0.9444	0.0280	0.0277	331.78	10.30
	0.9798	0.0103	0.0099	309.43	7.38
	0.9798	0.0103	0.0099	314.58	8.28
	0.9798	0.0103	0.0099	318.98	8.73
	0.9798	0.0103	0.0099	324.08	9.39
	0.9798	0.0103	0.0099	328.73	9.76
1:1 Acet/Isopr.					
	0.9822	0.0091	0.0087	309.53	7.43
	0.9822	0.0091	0.0087	314.98	8.05
	0.9822	0.0091	0.0087	319.20	8.73
	0.9822	0.0091	0.0087	324.03	9.61
	0.9822	0.0091	0.0087	328.78	9.97
	0.9939	0.0031	0.0030	307.73	7.48
	0.9939	0.0031	0.0030	314.73	7.86
	0.9939	0.0031	0.0030	318.33	8.59
	0.9939	0.0031	0.0030	324.15	8.83
	0.9939	0.0031	0.0030	328.35	9.67
	0.9948	0.0026	0.0025	309.88	7.92
	0.9948	0.0026	0.0025	314.28	8.03
	0.9948	0.0026	0.0025	318.70	8.45
	0.9948	0.0026	0.0025	323.30	9.24
	0.9948	0.0026	0.0025	328.30	9.59
	0.7668	0.1750	0.0582	309.58	5.90
	0.7668	0.1750	0.0582	314.95	6.78
	0.7668	0.1750	0.0582	320.83	8.16
	0.7668	0.1750	0.0582	325.20	7.92
	0.7668	0.1750	0.0582	329.50	8.41
3:1 Acet/Isopr.					
	0.7927	0.1556	0.0518	310.65	6.40
	0.7927	0.1556	0.0518	314.33	7.40
	0.7927	0.1556	0.0518	320.13	7.59

Volumetric ratio of organic solvents	x_{CO2}	$x_{acetone}$	$x_{isopropanol}$	T [K]	P[MPa]
	0.7927	0.1556	0.0518	324.88	7.98
	0.7927	0.1556	0.0518	328.85	8.43
	0.9052	0.0711	0.0237	310.63	7.24
	0.9052	0.0711	0.0237	314.78	7.70
	0.9052	0.0711	0.0237	319.40	8.20
	0.9052	0.0711	0.0237	323.82	8.81
	0.9052	0.0711	0.0237	329.80	9.69
	0.9181	0.0614	0.0204	308.88	7.41
	0.9181	0.0614	0.0204	317.38	8.26
	0.9181	0.0614	0.0204	320.42	8.61
	0.9181	0.0614	0.0204	325.48	10.30
	0.9181	0.0614	0.0204	329.55	11.51
	0.9512	0.0366	0.0122	309.83	7.77
	0.9512	0.0366	0.0122	315.53	8.71
	0.9512	0.0366	0.0122	320.60	9.77
3:1 Acet/Isopr.	0.9512	0.0366	0.0122	325.33	10.30
	0.9512	0.0366	0.0122	331.10	10.90
	0.9570	0.0323	0.0107	309.83	7.86
	0.9570	0.0323	0.0107	315.50	8.83
	0.9570	0.0323	0.0107	322.00	10.10
	0.9570	0.0323	0.0107	324.13	10.21
	0.9570	0.0323	0.0107	329.70	11.03
	0.9775	0.0169	0.0056	309.75	7.38
	0.9775	0.0169	0.0056	314.68	7.87
	0.9775	0.0169	0.0056	320.02	9.19
	0.9775	0.0169	0.0056	326.05	10.79
	0.9775	0.0169	0.0056	328.68	12.39
	0.9810	0.0143	0.0047	311.58	7.79
	0.9810	0.0143	0.0047	315.50	8.11
	0.9810	0.0143	0.0047	322.43	9.64
	0.9810	0.0143	0.0047	323.65	11.18
	0.9810	0.0143	0.0047	328.75	12.79
	0.9988	0.0009	0.0003	309.85	7.48
	0.9988	0.0009	0.0003	313.98	7.88
	0.9988	0.0009	0.0003	318.90	8.59
	0.9988	0.0009	0.0003	323.68	9.05
	0.9988	0.0009	0.0003	328.53	10.04

Volumetric ratio of organic solvents	x_{CO2}	$x_{acetone}$	$x_{isopropanol}$	T [K]	P [MPa]
3:1 Acet/Isopr.	0.9988	0.0008	0.0003	308.93	7.39
	0.9988	0.0008	0.0003	313.68	7.91
	0.9988	0.0008	0.0003	318.88	8.32
	0.9988	0.0008	0.0003	323.38	9.04
	0.9988	0.0008	0.0003	329.12	9.87
5:1 Acet/Isopr.	0.7129	0.2401	0.0471	308.95	5.42
	0.7129	0.2401	0.0471	315.55	6.57
	0.7129	0.2401	0.0471	319.58	6.58
	0.7129	0.2401	0.0471	323.88	6.83
	0.7129	0.2401	0.0471	330.05	8.19
	0.7499	0.2091	0.0410	309.72	5.62
	0.7499	0.2091	0.0410	315.05	7.07
	0.7499	0.2091	0.0410	320.38	8.20
	0.7499	0.2091	0.0410	325.02	7.52
	0.7499	0.2091	0.0410	329.75	8.04
	0.8961	0.0877	0.0162	308.68	6.77
	0.8961	0.0877	0.0162	314.72	7.67
	0.8961	0.0877	0.0162	320.38	9.12
	0.8961	0.0877	0.0162	324.08	10.09
	0.8961	0.0877	0.0162	329.70	10.48
	0.9100	0.0760	0.0140	308.72	6.91
	0.9100	0.0760	0.0140	314.55	7.79
	0.9100	0.0760	0.0140	319.58	8.28
	0.9100	0.0760	0.0140	323.85	9.09
	0.9100	0.0760	0.0140	329.05	10.65
	0.9368	0.0534	0.0098	308.87	7.18
	0.9368	0.0534	0.0098	314.08	7.90
	0.9368	0.0534	0.0098	319.55	8.81
	0.9368	0.0534	0.0098	324.33	9.71
	0.9368	0.0534	0.0098	329.35	10.70
	0.9454	0.0461	0.0085	310.20	8.89
	0.9454	0.0461	0.0085	315.75	8.89
	0.9454	0.0461	0.0085	319.13	9.17
	0.9454	0.0461	0.0085	324.15	9.95
	0.9454	0.0461	0.0085	329.70	10.76
	0.9759	0.0203	0.0037	309.08	7.58
	0.9759	0.0203	0.0037	316.18	8.56

Table 5. Average data of the redissolution points for each composition (5/5)

Volumetric ratio of organic solvents	x_{CO2}	$x_{acetone}$	$x_{isopropanol}$	T [K]	P [MPa]
	0.9759	0.0203	0.0037	319.55	9.06
	0.9759	0.0203	0.0037	324.55	10.33
	0.9759	0.0203	0.0037	328.63	11.16
	0.9796	0.0172	0.0032	312.13	8.34
	0.9796	0.0172	0.0032	314.68	8.73
	0.9796	0.0172	0.0032	319.33	9.41
	0.9796	0.0172	0.0032	324.18	11.21
	0.9796	0.0172	0.0032	329.83	11.95
	0.9938	0.0050	0.0011	310.08	7.45
	0.9938	0.0050	0.0011	314.40	8.14
	0.9938	0.0050	0.0011	318.38	8.61
	0.9938	0.0050	0.0011	323.55	9.04
	0.9938	0.0050	0.0011	328.60	9.62

An analysis of these data reveals some of the following characteristics of the system. Firstly, from the raw data, the redissolution points have a higher pressure than the opacity points observed at the same composition and temperature. The difference is usually about 0.3 or 0.4 MPa, although for a 3:1 ratio of acetone/isopropanol this difference is increased especially at higher temperatures. The most likely reason for the difference is visual observation itself. It is useful to plot the P-T diagrams for each of the ratios to see this and other aspects. Thus, in Figure 7, the temperature range of the study is plotted on the horizontal axis and the measured pressure data on the vertical axis. Each of the colours represents the carbon dioxide composition in mole fraction. The volumetric ratio of acetone and isopropanol is 1:1. The opacity points are represented by circles while the redissolution points are represented by triangles. The diagram shows how the pressure characterising phase transition increases as the temperature inside the cell increases. On the other hand, it is true that, up to a carbon dioxide mole fraction of approx. 0.8930, when more carbon dioxide is added to the cell, the measured pressures are higher, although this tendency does not always occur, especially when comparing some of the redissolution points. For example, for a mole fraction of 0.8930 CO_2 (shown in red) the pressure of the dissolution points at approx. 330 K is higher than for mole fractions higher than this.
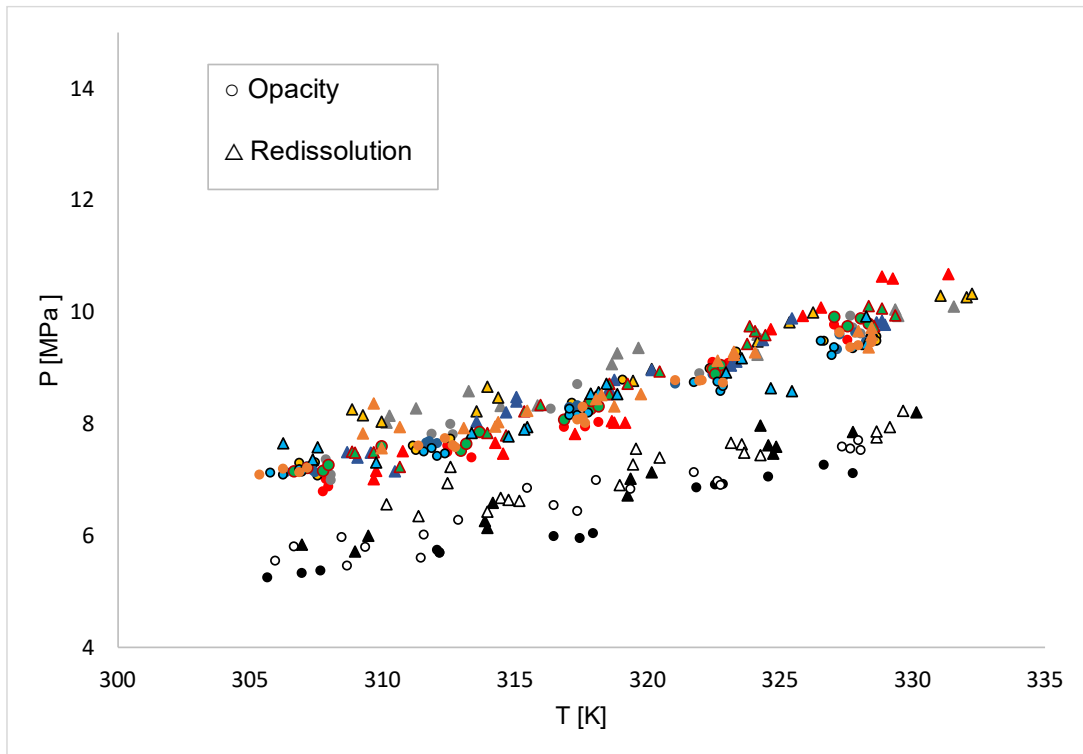
CO$_2$ mole fraction	Colour legend
0.7118	⬛
0.7491	⬜
0.8930	🟥
0.9351	⬜ (grey)
0.9444	🟨
0.9798	🟦 (dark blue)
0.9822	🟩
0.9939	🟦 (light blue)
0.9948	🟧

Figure 7. P-T diagram for a 1:1 volumetric acetone/isopropanol ratio.

The same representation is carried out for a 3:1 ratio and is shown in Figure 8. The pressures reached for this ratio are higher than for the 1:1 ratio and this effect is particularly noticeable at temperatures above 320 K. The trend is still linear even though the data is more scattered and more disordered, probably due to possible errors in experimentation such as the inherent error of visual observation or the difficult visual assessment of turbidity and clarity at high temperatures.
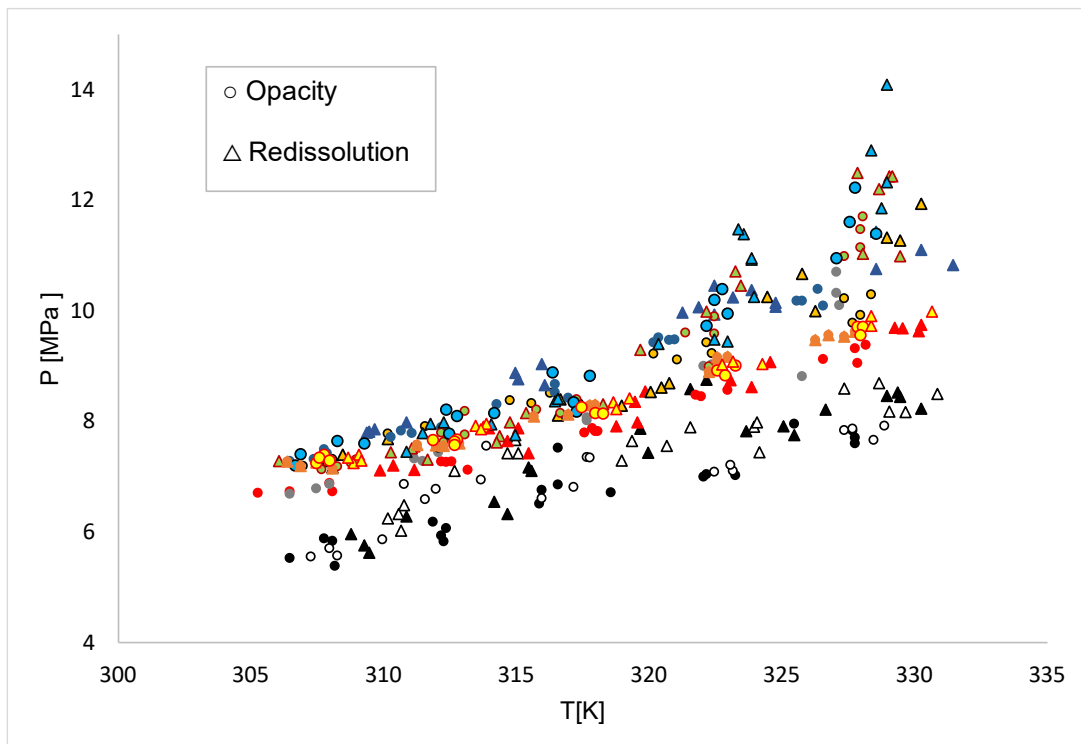
CO$_2$ mole fraction	Colour legend
0.7668	
0.7926	
0.9052	
0.9181	
0.9512	
0.9570	
0.9752	
0.9810	
0.9987	
0.9988	

Figure 8. P-T diagram for a 3:1 volumetric acetone/isopropanol ratio.

For the 5:1 acetone/isopropanol volumetric ratio, the P-T diagram is shown in Figure 9. Again, there is a linear trend in the cloud point and redissolution point pressures with temperature.
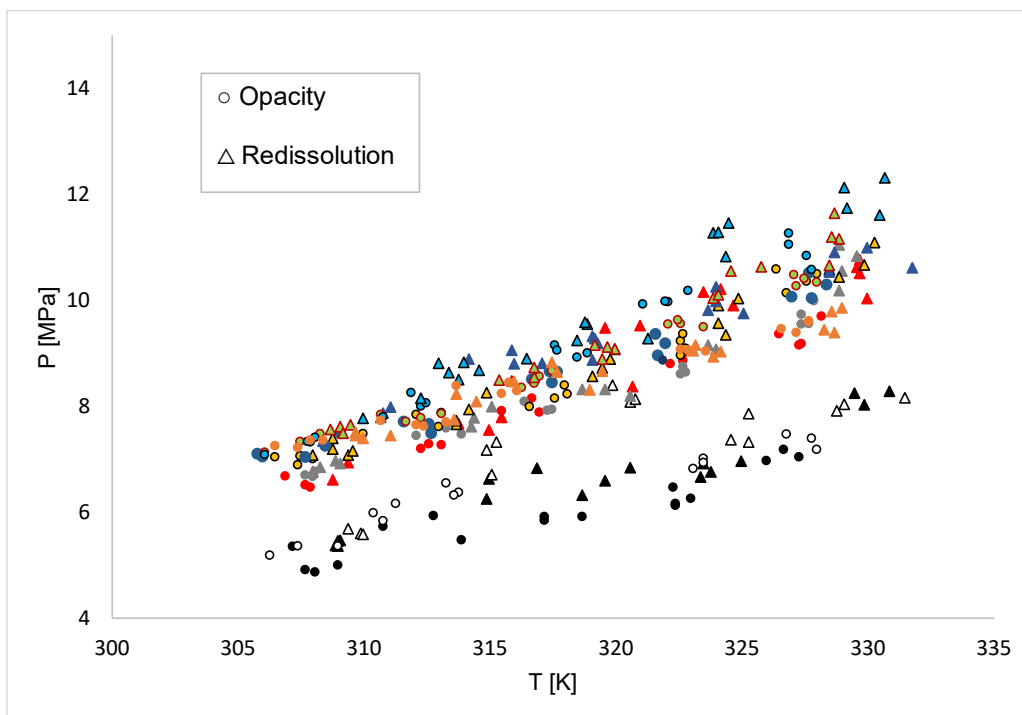
CO$_2$ mole fraction	Colour legend
0.7128	■ (black)
0.7499	□ (white)
0.8961	■ (red)
0.9099	■ (grey)
0.9368	■ (yellow)
0.9454	■ (dark blue)
0.9759	■ (green)
0.9796	■ (light blue)
0.9938	■ (orange)

Figure 9. P-T diagram for a 5:1 acetone/isopropanol ratio.

The three figures above have been scaled equally to make a comparison between the three ratios. In general, the dispersion of the data is greater when the proportion of acetone is increased. However, for a 3:1 acetone/isopropanol ratio, a higher scatter is clearly observed. This fact mentioned above probably stems from the different ability to visually observe a transparent phase becoming opaque and the disappearance of the last traces of opacity. Despite this, it has not been considered for any of the three ratios that there is significant hysteresis between the opacity and redissolution points, so I therefore decided to study the opacity and redissolution data together. Furthermore, it is observed that for all experiments and in all temperature ranges the cloud point pressure increases with temperature, indicating that there is no temperature inversion for the mixture. Another observation that is common to all three ratios is that although there is an increase in

40

pressure with temperature, for a composition of around 0.99 (shown in orange and yellow in the diagrams) and corresponding to the addition of 0.25 mL volumes of mixture, there is a decrease in the observed pressures. If the pressure-composition (CO_2 mole fraction at given organic solvent ratios at constant temperature) graph were plotted, it would have a slightly quadratic form. However, there are multiple different carbon dioxide mole fractions in each of the three figures, which exhibit very similar pressure–temperature tendencies. Looking at these data with very similar cloud-point and redissolution pressures, one may suspect that the measurements were carried out in the close vicinity of the mixture-critical point.

Also, it is remarkable that for some compositions (for example, $x\_CO_2 = 0.8930$ in the measurements with a 1:1 acetone/isopropanol ratio or $x\_CO_2 = 0.9512$ in the measurements with a 3:1 acetone/isopropanol ratio) with a lower proportion of carbon dioxide, the redissolution pressures at a given temperature achieved are higher than for those with a higher proportion. Redissolution was not clearly visible at a qualitative level, especially at temperatures of 318.15 K and above.

When analysing the diagrams, it is useful to consider what the effect of different mixtures may be for e.g., anti-solvent purposes. For example, one of the factor's directly influencing solubility is the molecular weight of the compounds. The lower the molecular weight of the compound, the higher its solubility in SCF (Latsky et al. 2020). In this case the molecular weight of acetone is 58.08 g/mol and that of isopropanol is 60.1 g/mol. The addition of isopropanol would result in a reduction in solubility, so higher cloud-redissolution point pressures might be expected at the same temperature if the ratio is pushed towards isopropanol. This is not apparent in the diagrams above. Looking at the experimental data, the difference in molecular weights is very small and does not seem to be a reason that seems to clearly influence the measured pressure. The different functional groups that are present in the two organic solvents probably largely distort the effect one would expect based on their similar molar masses.

Complementing data processing, an analysis can be carried out from an empirical mathematical point of view to describe the system and avoid, for example, future experimentation. For this reason, the surface graphs were obtained based on different types of fitting. While neither of the applied functions has a physical-chemical background they are easy to use and require no computational tools other than commonly available software with spreadsheet capabilities. Version 13 of Statistica™ software

(TIBCO Software Inc.) is used to process the data and to obtain some of the fittings and graphs that will be seen in this section.

Generally, the three ratios studied respond correctly to a linear fit, especially for lower carbon dioxide compositions. Linear functions are of course the simplest to describe the effects of experimental parameters, in this case temperature and the mole fraction of carbon dioxide on the cloud- and redissolution pressure.

If the surfaces are fitted linearly, the behaviour can be described as follows:

$$P[MPa] = A \cdot x_{CO_2} + B \cdot T[K] + C \qquad [\ 8.]$$

A, B are the coefficients along the constant C that represent the behaviour of the system and are shown in Table 6.

Table 6. Linear fitting results of the cloud point pressure as a function of the x_CO_2 and temperature.

Acetone/Isopropanol volumetric ratio	A	B	C	R^2
1:1	6.791	0.1183	-35.7293	0.9439
3:1	8.7346	0.1586	-50.1104	0.9036
5:1	9.6619	0.1532	-49.1809	0.9462

From this fit, the R^2 coefficient is not too high for the 3:1 ratio of acetone and isopropanol, probably due to the difference in opacity and redissolution pressures observed at temperatures of 50 and 55 ℃ and because of the curvature that we experienced in the region of the mixture-critical point. Linear fits are represented for the three study ratios in Figure 10, Figure 11 and Figure 12.
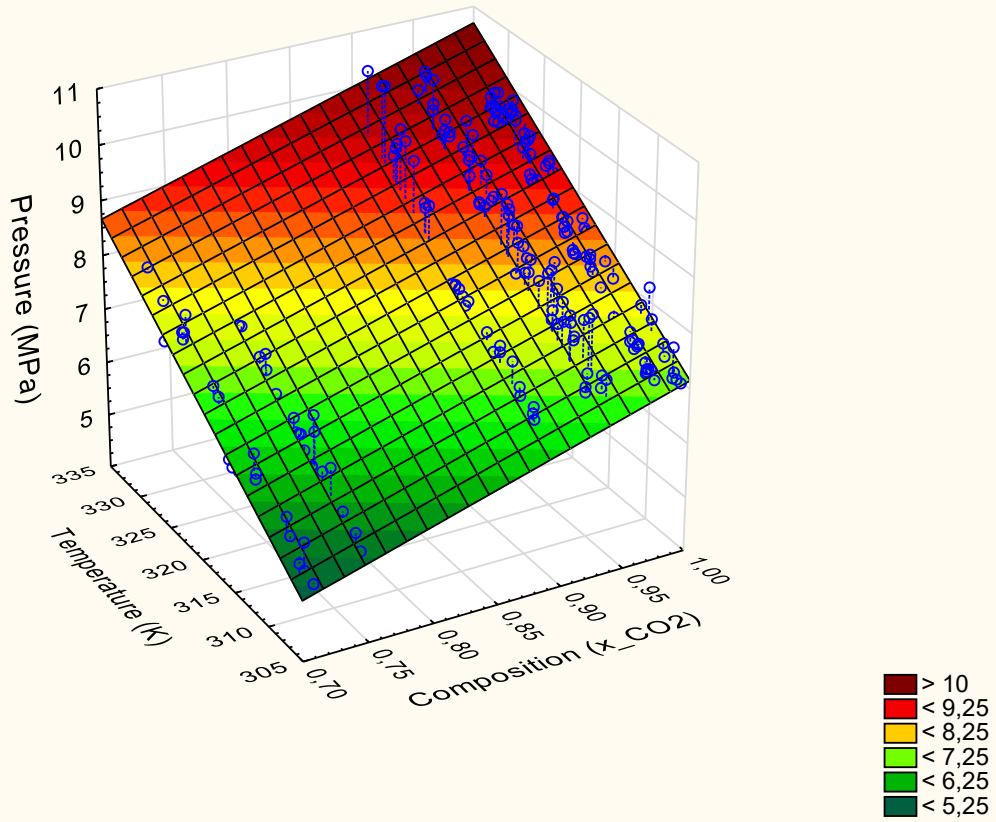
Figure 10. Linear surface graph for measurement results with a 1:1 volumetric ratio of acetone/isopropanol.
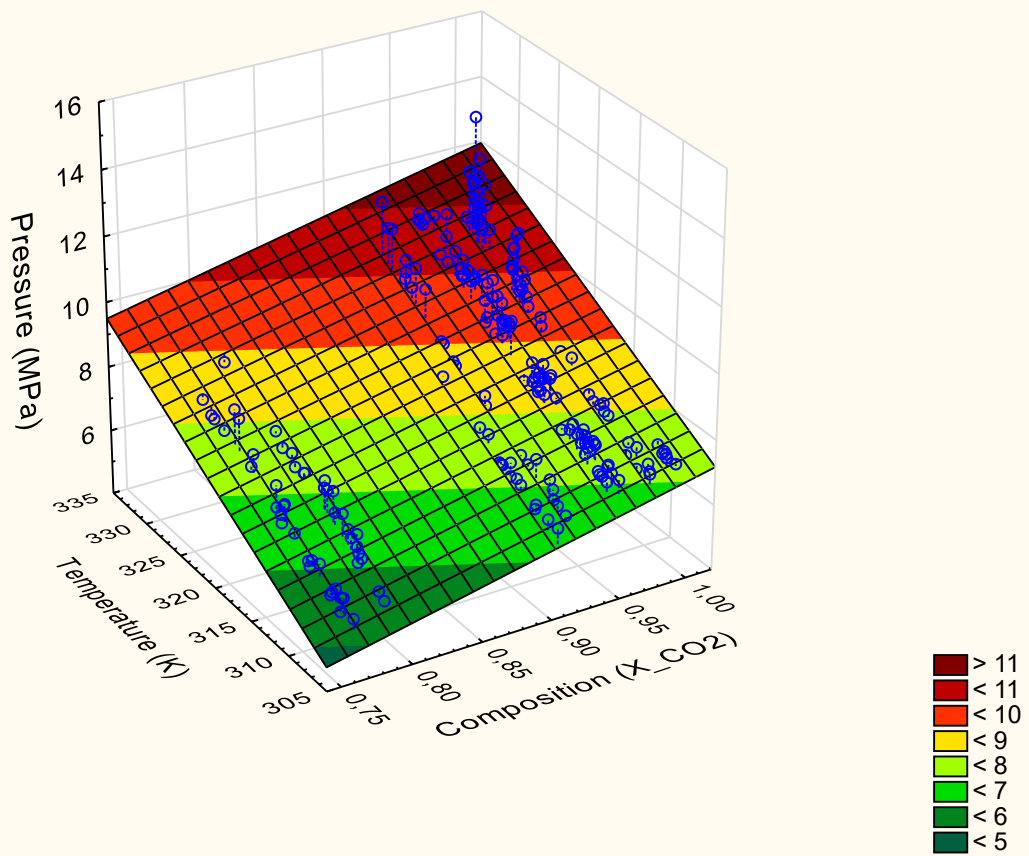
Figure 11. Linear surface graph for measurement results with a 3:1 volumetric ratio of acetone/isopropanol.
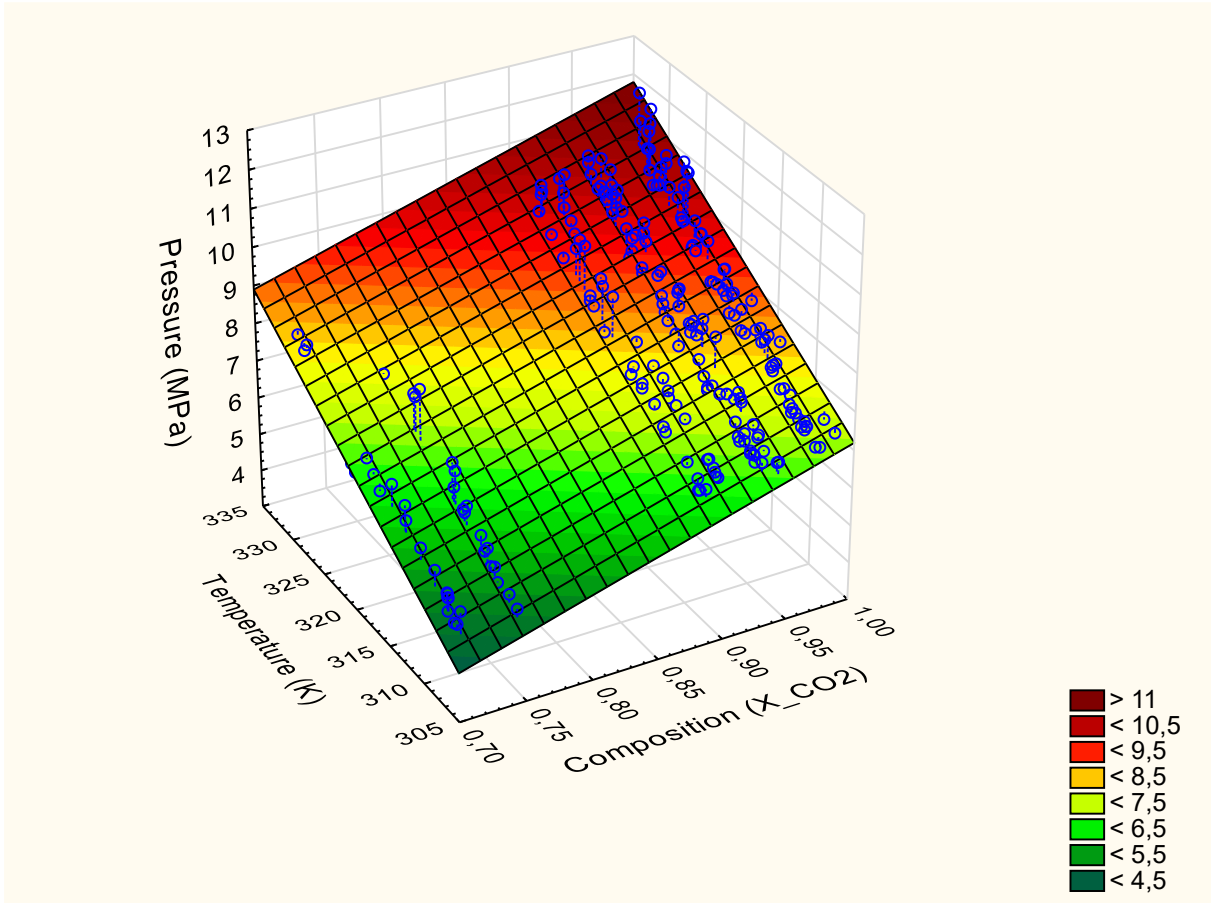
Figure 12. Linear surface graph for measurements with a 5:1 volumetric ratio of acetone/isopropanol.

At higher carbon dioxide mole fractions (beyond approx. *x_CO2 = 0.95*) the tendency of cloud and redissolution point pressures at a given temperature against the mole fraction of carbon dioxide shows a trend with a maximum. This indicates that the measurements were conducted in the vicinity of the mixture-critical points. This fact could already be sensed in Figure 7, Figure 8 and Figure 9, where the datasets corresponding to the above-mentioned compositions could hardly be distinguished but is more apparent in the surface diagrams.

The quadratic fitting was necessary because of this apparent curvature of the pressure-composition tendency in the areas close to the critical point. As stated before, although the quadratic function follows the tendency of the measurement points with respect to the curvature, the thermodynamic aspect of phase separation is still not taken into consideration. The general form of the fitted quadratic function can be described as follows:

$$P[MPa] = A \cdot x_{CO_2}^2 + B \cdot T[K]^2 + C \cdot x_{CO_2} \cdot T[K] + D \cdot x_{CO_2} + E \cdot T[K] + F \qquad [9.]$$

In this case, there are 5 coefficients and a constant that determine the quadratic function, as shown in Table 7.

Table 7. Quadratic fitting results of the cloud point pressure as a function of the x_CO2 and temperature.

Acetone/Isopropanol volumetric ratio	A	B	C	D	E	F
1:1	-37.9685	0.0009	0.0487	56.456	-0.5081	43.7562
3:1	-37.6677	0.0021	0.3181	-26.0403	1.446	223.2199
5:1	-20.5203	0.0009	0.213	-23.133	-0.6396	93.0408

Quadratic fits are represented for the three study ratios in Figure 13, Figure 14 and Figure 15.
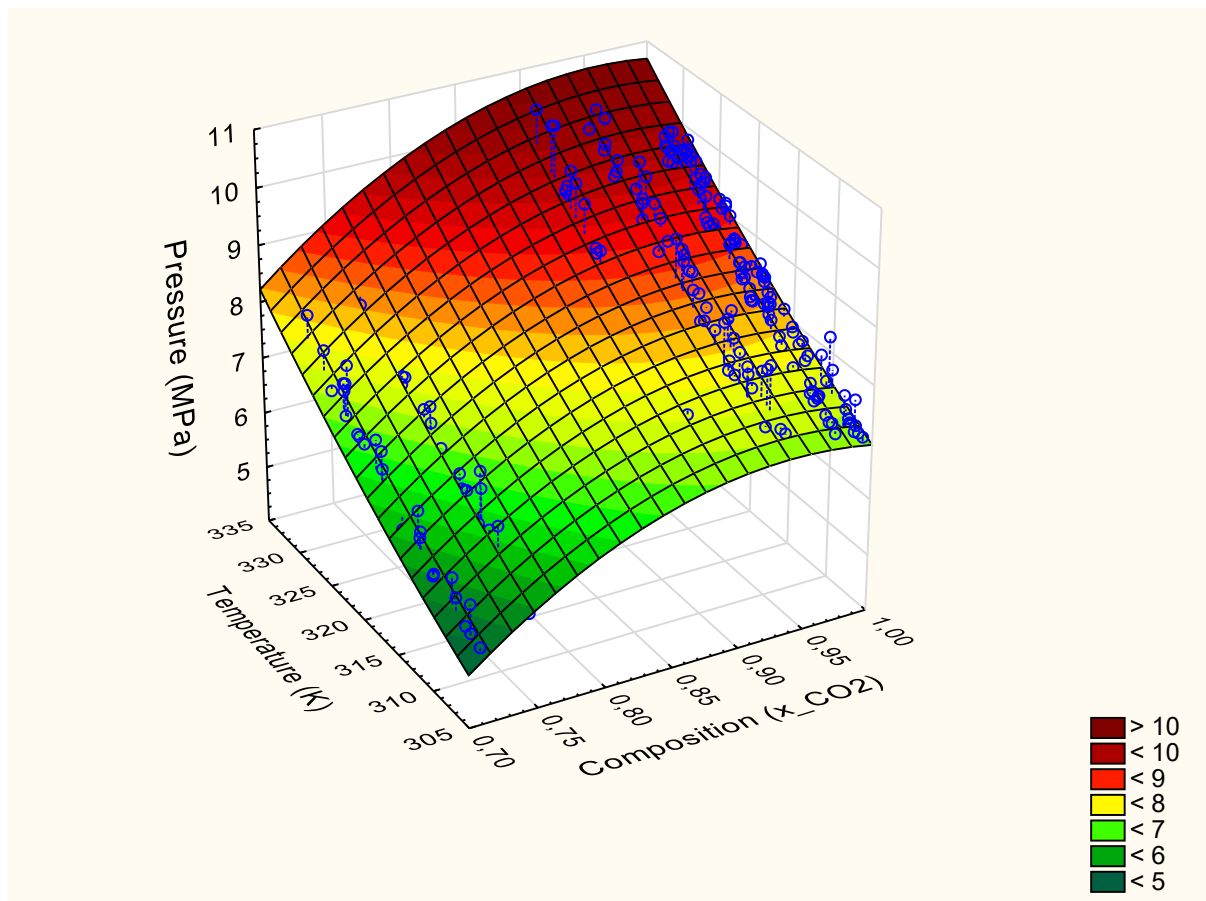
Figure 13. Quadratic surface graph for 1:1 volumetric ratio of acetone/isopropanol.
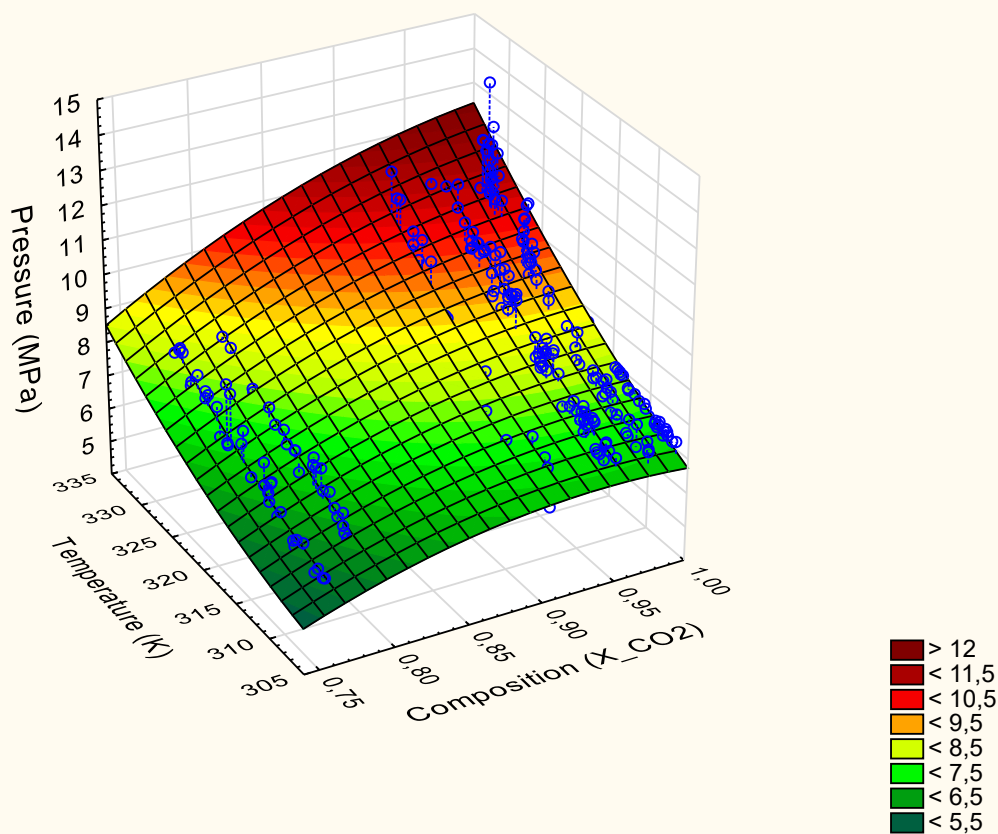
Figure 14. Quadratic surface graph for 3:1 volumetric ratio of acetone/isopropanol.
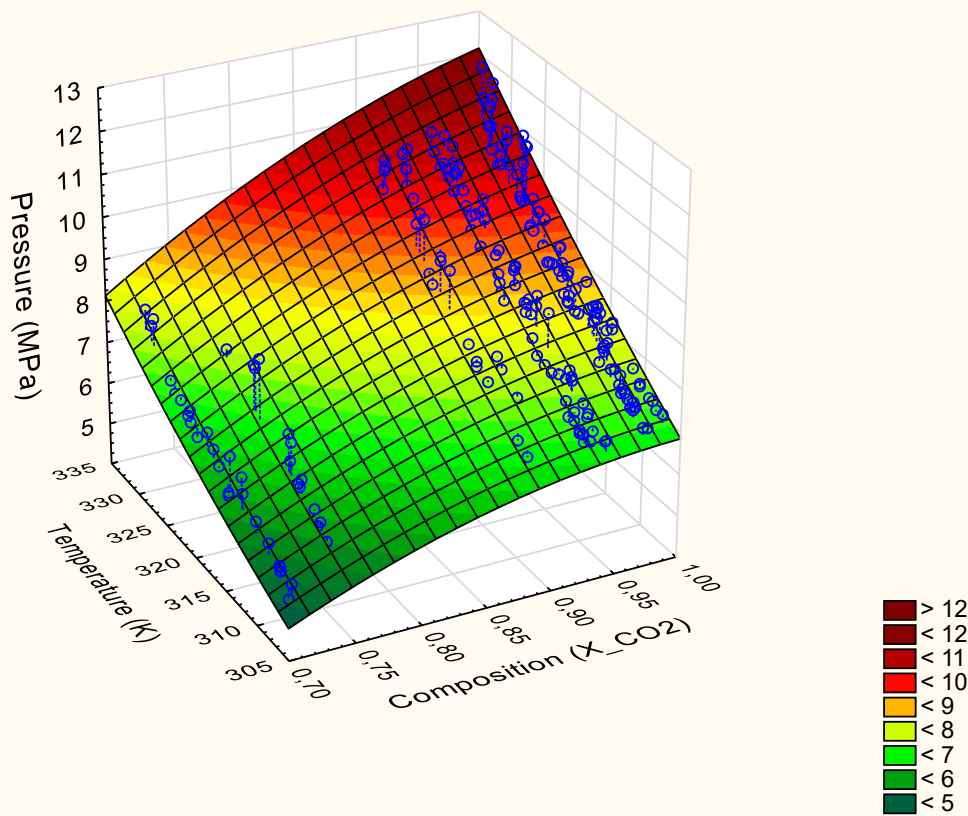
Figure 15. Quadratic surface graph for 5:1 volumetric ratio of acetone/isopropanol.

The fitted, simple equations may be used to approximate the pressure needed to form a homogeneous mixture knowing the desired composition and temperature of the system.

4.2. Thermodynamic modelling

The Aspen Plus V.10 © programme is used to model the behaviour of the phase data measured in this work. The aim of the Aspen data processing is to find the binary interaction parameters between the pairs of components by regressing the experimentally obtained data. Although in this work we have a ternary mixture, often, the parameters obtained from binary mixtures can be adapted to ternary systems unaltered or by adding some modification. Table 1 in the literature section 2.4 presents the main parameters found for the carbon dioxide + organic solvent systems. Comparison of these parameters can be carried out depending on whether the EOS and mixing rule used in the modelling are the same as that found in the literature. In case this does not happen, the BIPs reported in those articles cannot be combined but have to be re-adjusted with the simple mixing rules used by the modelling EOS. It should also be noted that the new BIPs obtained in the modelling of the ternary system do not necessarily describe the behaviour of the binary mixtures and should therefore be checked for their proper use.

The thermodynamic models used in this work are Peng-Robinson (PR) and Soave-Redlich-Kwong (SRK) cubic equations of state. The PR EOS has been used in many articles with supercritical CO_2 and acetone/isopropanol (Bamberger and Maurer 2000; Wu et al. 2004; Lei et al. 2012) and where it was concluded that this equation correlated correctly with the experimental data. SRK EOS has also been used for this purpose (Radosz 1986). Both equations are therefore models that correctly describe the behaviour of multicomponent systems, although their origin was focused on the study of hydrocarbon systems. The aim of this paper is to see whether the correlation with these two EOS is also able to describe the system appropriately.

The Peng-Robinson cubic equation of state (Peng-Robinson 1976) is defined as:

$$P = \frac{RT}{V_m - b} - \frac{a}{V_m(V_m + b) + b(V_m - b)}$$

[10.]

The pressure P (Pa = J/m^3) is determined from the absolute temperature T (K) and molar volume V_m (m^3/mol). R is the universal gas constant (J/mol K). The attraction parameter a (J·m^3 /mol^2) is a function of the temperature of the mixture (T), the critical

47

temperature (T_c), the critical pressure (P_c), and the acentric factor (ω) of the compounds. Parameter b (van der Waals covolume) (m^3/mol) is a function of the critical temperature and critical pressure of the compounds in the mixture. The Aspen programme uses this function based on the parameters presented below:

$$a = \sum_i \sum_j x_i x_j \left(a_i a_j\right)^{0.5} \left(1 - k_{ij}\right) \qquad [11.]$$

The temperature dependence of the parameter a can be expressed based on the parameter k_{ij} as follows:

$$k_{ij} = k_{ij}^{(1)} + k_{ij}^{(2)} T + \frac{k_{ij}^{(3)}}{T} \qquad [12.]$$

The dependence of a on temperature is given not only by the interaction parameter k_{ij}:

$$a_i = f\left(T, T_{c_i}, P_{c_i}, \omega_i\right) \qquad [13.]$$

$$a_i(T) = a(T_c) \cdot \alpha(T_r, \omega) \qquad [14.]$$

The particularised parameter a at the critical point can be expressed as:

$$a_i(T_c) = 0.45724 \frac{R^2 T_c^{\,2}}{P_c} \qquad [15.]$$

In equation [14.] the parameter α depends on the reduced temperature (T_r) and a characteristic constant for each compound (κ):

$$\alpha^{1/2} = 1 + \kappa\left(1 - T_r^{\,1/2}\right) \qquad [16.]$$

The reduced temperature T_r is calculated as:

$$T_r = \frac{T}{T_c} \qquad [17.]$$

Where κ is a constant characteristic of each compound:

$$\kappa = 0.37464 + 1.54226\omega - 0.26992\omega^2 \qquad [18.]$$

In equation [18.], the letter ω denotes the acentric factor of the component i. The parameter b depends on the composition as follows:

$$b = \sum_i x_i b_i \qquad [19.]$$

The temperature dependence of b can be expressed as follows:

$$b_i = f\left(T_{c_i}, P_{c_i}\right) \tag{[20.]}$$

$$b(T) = b(T_c) \tag{[21.]}$$

The particularised parameter b at the critical point can be expressed as:

$$b(T_c) = 0.07780\frac{RT_c}{P_c} \tag{[22.]}$$

It can be seen from these equations how the critical parameters of each of the compounds are basic for the modelling of the mixture. In this sense, it is worth comparing the data used by Aspen by default with some literary reviews where these parameters have also been obtained (Table 8). Although some differences can be discovered among the values obtained from different sources, these can be considered minor, and the default values of Aspen Plus may be accepted and used in the calculations.

Table 8. Critical properties and acentric factor for pure compounds.

Compound	Tc [K]	Pc[bar]	ω	Reference
2-propanol	508.30	47.63	0.665	*(Khoiroh and Lee 2011)*
	508.31	47.64	0.669	*(Dell'Era et al. 2007)*
	508.30	47.62	0.665	*(Poling et al. 2001)*
	508.26	47.50	0.664	*Default Value Aspen Plus V.10*
2-propanone	508.10	47.00	0.305	*(Bamberger and Maurer 2000)*
	508.10	47.00	-	*(Melhem et al. 1989)*
	508.06	47.05	0.308	*Default Value Aspen Plus V.10*
CO_2	304.20	73.90	0.213	*(Bamberger and Maurer 2000)*
	304.13	73.77	0.224	*(Span and Wagner 1996)*
	304.16	73.81	0.225	*Default Value Aspen Plus V.10*

The binary interaction parameters between the pairs of components that serve as the basis for the regression are sought in the literature. In the found papers, the interaction parameters were only present in binary systems formed from the component pairs discussed in this work. The binary parameters found using the PR EOS and classical mixing rules of this equation as in this modelling, reported a carbon dioxide-acetone

49

interaction parameter -0.03 (Wu et al. 2004) and 0.007 (Lei et al. 2012). The carbon dioxide-isopropanol parameter was 0.128. (Galicia-Luna y Elizalde-Solis 2010). No literature data were found for the interaction between acetone and isopropanol. Other articles using modified PR as the equation of state and the Panagiotopoulos and Reid mixing rule reported a CO_2/acetone interaction parameter of -0.0251 and CO_2/isopropanol of 0.1467 (Bamberger and Maurer 2000). As the mixing rule applied in the current study is different, these values cannot be directly used in the current simulation. The binary interaction parameters should be re-fitted to the already existing measurement data of the other authors. However, such values may need to undergo modification to be used to appropriately describe the behaviour of the ternary system. In Aspen, this binary interaction is defined as PRKBV-1. On the other hand, it should be noted that symmetrical parameters between the pairs have been considered as in *Lei et al. 2012* and *Wu et al. 2004* . In *Bamberger and Maurer 2000* were not considered symmetrical, with the parameters acetone/CO_2 of -0.0008 and isopropanol/CO_2 of 0.1005.

As the amount of measured phase equilibrium data is significant, I decided to use the regression function of the process simulator to determine binary interaction parameters and extend their applicability through including the temperature-dependence using their second and third elements (see equation *[12.]*).

The process followed to carry out the regression takes as initial values the binary parameters found in the literature (Wu et al. 2004; Galicia-Luna and Elizalde-Solis 2010) takes as upper and lower limits +10 and -10 respectively. The objective function is rotated with the Maximum-Likelihood estimation and the algorithm of minimization is the Britte-Luecke algorithm.

The problem with cubic equations of state is that they do not correctly describe those points that are close to the critical point of the mixture. Near the mixture critical point, the estimation of the molar volume becomes inaccurate. Together with the measurement error, this may result in the incapability of solving the phase equilibrium problem. In this case, this occurs when the CO_2 mole fraction takes values higher than approximately 0.95. In practical terms, the simulation programme presents errors and warnings when these points are included, and the residual error values obtained are also higher. For this reason, only compositions that avoid such problems (<0.95) were included in the data to be regressed. As a result, a filtering of the experimental data was carried out, reducing the number of points included in the programme to around 300, which corresponds to the range of compositions. The opacity and redissolution data were treated together, although

the difference between them cause the root mean square error (RMSE) of the regression to increase.

$$RMSE = \left[\sum_{i=1}^{N} \left(x_{exp} - x_{est} \right)^2 \Big/ N \right]^{1/2}$$

Where:

$\left(x_{exp} - x_{est} \right)^2$ is the quadratic difference between the measured value and the estimated value in the regression and N the total number of values in the regression.

Table 9 shows the results obtained for the regression with PR when the temperature dependence is not considered ($k_{ij} = k_{ij}^{(1)}$):

Table 9. Binary parameters obtained from the regression with Aspen. Peng Robinson equation of state.

	CO2-Acet.	CO2-Isopr.	Acet.-Isopr.	RMSE
$k_{ij}^{(1)}$	-0.0214	-0.1001	-0.2460	12.78

The P-T diagram was constructed for one of the studied compositions to see if there is a real difference between considering or not considering BIPs. The composition for which this analysis is carried out is *x_CO₂ = 0.7491*; *x_acet = 0.1285*; *x_isoprop = 0.1224*. Figure 16 and Figure 17 show the differences of fit obtained for the data studied.

Figure 16. P-T diagram for the PR model with the BIPs (non-temperature dependant).

x_CO₂ = 0.7491; x_acet = 0.1285; x_isoprop = 0.1224. BIPs CO₂/Acetone: -0.0214; CO₂/Isopropanol: -0.1001; Isopropanol/Acetone: -0.2460

The circles represent the opacity points while the crosses represent the redissolution points.
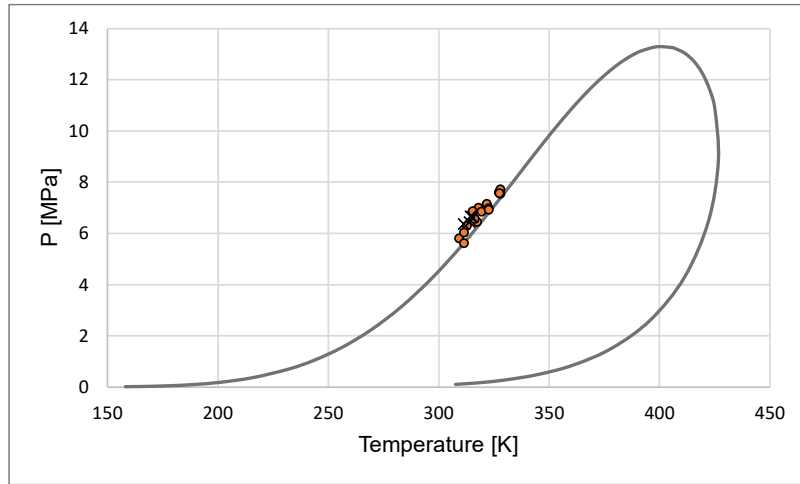
Figure 17. P-T diagram for the PR model with the BIPs=0.

x_CO$_2$ = 0.7491; x_acet = 0.1285; x_isoprop = 0.1224.

By adding the values for the interaction parameters, the fit with respect to the PR model is more correct than for the case where regression was carried out setting all BIPs to 0.

The next step is to add the temperature dependence to the regression to see whether it influences the fit. The dependence of the parameter k_{ij} on temperature is shown in *[13.]*.

There are now 9 parameters to be regressed, which are $k_{ij}^{(1)}$, $k_{ij}^{(2)}$ and $k_{ij}^{(3)}$ corresponding to each pair of compounds. The process carried out is the same, however, it is observed that the parameter $k_{ij}^{(2)}$ has a much smaller influence on k_{ij}, than the parameter $k_{ij}^{(3)}$ and the limits assigned to the regression have an influence. The regression is tested with upper and lower bounds of +10 and -10 and +1000 and -1000, since both results offer values that could be acceptable. However, it is observed that when the limits are lower, the parameter k_{ij} obtained by assigning different temperatures is more similar to the parameter obtained without temperature dependence and that they are closer to the previously mentioned literary values. The values with a range at the lower limits are therefore chosen (Table 10).

Table 10. Binary parameters for Peng Robinson's model. Temperature dependence.

	CO2-Acet.	CO2-Isopr.	Acet.-Isopr.	RMSE
$k_{ij}^{(1)}$	0.1922	0.3671	-0.4159	
$k_{ij}^{(2)}$ *[1/K]*	-0.0008	-0.0015	0.0006	12.46
$k_{ij}^{(3)}$ *[K]*	10	3.4470	-8.2567	

A check can be made at this point to see how the variation of the parameter k_{ij} is for each pair of compounds with respect to the temperature range applied in this study (Table 11). The parameters obtained for the CO_2-acetone interaction are certainly close to the literature value of -0.03 (Wu et al. 2004) while the same is not true for the CO_2-isopropanol interaction (0.128) (Galicia-Luna and Elizalde-Solis 2010).

Table 11. Dependence of binary parameters on temperature for the PR model.

Temperature (K)	$k_{CO2-acet.}$	$k_{CO2-isopr.}$	$k_{acet-isopr.}$
303.15	-0.0124	-0.0849	-0.4431
308.15	-0.0130	-0.0928	-0.4427
313.15	-0.0135	-0.1006	-0.4422
318.15	-0.0140	-0.1084	-0.4418
323.15	-0.0145	-0.1162	-0.4414
328.15	-0.0149	-0.1240	-0.4410

Visually, the P-T-diagram is performed again to see if there is a temperature dependence in the fitting (Figure 18).
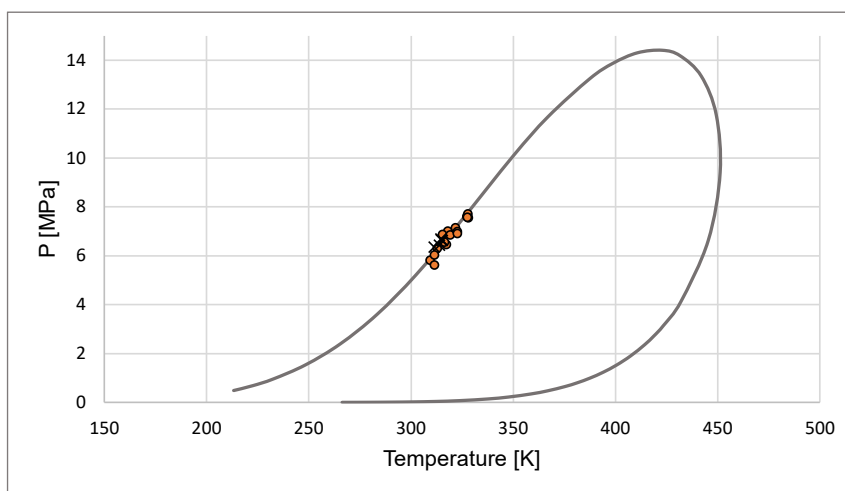
Figure 18. P-T diagram for the PR model with the BIPs (temperature dependant).

x_CO₂ = 0.7491; x_acet = 0.1285; x_isoprop = 0.1224.

Compared to Figure 16, it appears that the new fit better models the points at a higher temperature for the composition under study.

Figure 19 shows how the model behaves when using the BIPs obtained from the regression with +1000 and -1000 bounds. It can be seen that the modelling does not correctly describe the behaviour of the system over the whole range of temperatures and pressures at a given composition.
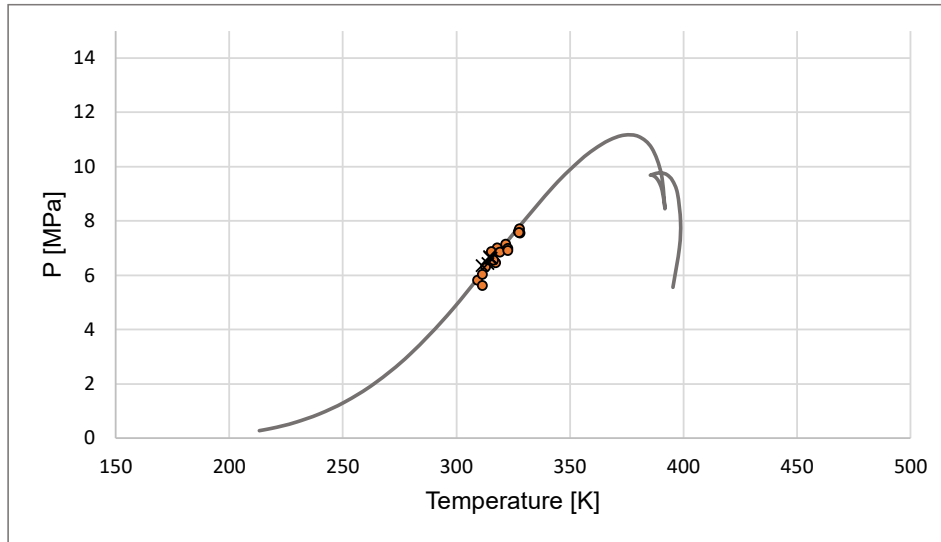
Figure 19. P-T diagram for the PR model with BIPs obtained when limits are relaxed (temperature dependant).

x_CO₂ = 0.7491; x_acet = 0.1285; x_isoprop = 0.1224.

An identical process is followed for the SRK thermodynamic model (Soave 1971) which is defined as follows:

$$P = \frac{RT}{V_m - b} - \frac{a}{V_m(V_m + b)}$$

[24.]

The parameter a is defined differently this time than in the case of Peng Robinson:

$$a = \sum_{i=1}^{n} \sum_{j=1}^{n} x_i x_j \sqrt{a_i a_j} (1 - k_{ij})$$

[25.]

The particularised parameter a at the critical point can be expressed as:

$$a_i(T_c) = 0.42747 \frac{R^2 T_c^2}{P_c}$$

[26.]

Equations *[14.]* and *[16.]* concerning the α parameter are the same as PR EOS while κ changes:

$$\kappa = 0.480 + 1.574\omega - 0.176\omega^2$$

[27.]

The parameter b depends on the composition as follows:

$$b = \sum_i x_i b_i$$

[28.]

54

The particularised parameter b at the critical point changes and can be expressed as:

$$b(T_c) = 0.08664 \frac{RT_c}{P_c}$$

<div align="right">[29.]</div>

The binary interaction parameters k_{ij} for this model are defined as SRKKIJ-1. No binary parameters for this thermodynamic model were found in the literature that could serve as a reference for the regression, so a value of 0 was used as initial guess. The parameter k_{ij} obtained from the regression for the SRK thermodynamic model are shown in Table 12:

Table 12. Binary parameters obtained from the regression with Aspen. SRK model.

	CO2-Acet.	CO2-Isopr.	Acet.-Isopr.	RMSE
$k_{ij}^{(1)}$	0.0352	0.0638	0.0178	16.64

When the regression is done with the temperature dependence for the parameter k_{ij}, it is observed that the second term has no influence again. The resulting fit is worse than for the PR case with the RMSE being higher. However, at the graphical level, no noticeable differences with Figure 18 are observed, so it has not been included. For this case, no influence on the variation of the limits for the third term is denoted.

The binary parameters of temperature dependence are shown in Table 13.

Table 13. Binary parameters obtained from the regression with Aspen. SRK model. Temperature dependence.

	CO2-Acet.	CO2-Isopr.	Acet.-Isopr.	RMSE
$k_{ij}^{(1)}$	0.0037	0.0234	0.0026	
$k_{ij}^{(2)}$	0	0	0	16.42
$k_{ij}^{(3)}$	3.3638	6.9543	-0.0113	

Table 14 shows the result of the binary parameters for the studied temperature range and for the SRK model.

Table 14. Dependence of binary parameters on temperature for the SRK model.

Temperature (K)	$k_{CO2-acet.}$	$k_{CO2-isopr.}$	$k_{acet-isopr.}$
303.15	0.0154	-0.0849	-0.4431
308.15	0.0152	-0.0928	-0.4427
313.15	0.0151	-0.1006	-0.4422
318.15	0.0149	-0.1084	-0.4418
323.15	0.0147	-0.1162	-0.4414
328.15	0.0146	-0.1240	-0.4410

For the SRK model, if the temperature dependence is introduced, the results obtained for the parameters differ more with respect to the non-temperature dependence. In this sense, a different behaviour of the model could be expected, so the P-T diagram has been plotted again for the composition of $x\_CO_2 = 0.7491$; $x\_acet = 0.1285$; $x\_isoprop = 0.1224$ (Figure 20 and Figure 21).
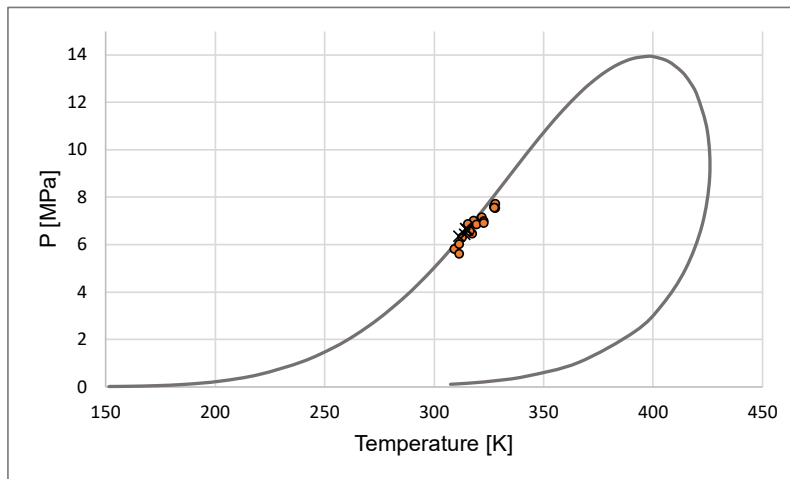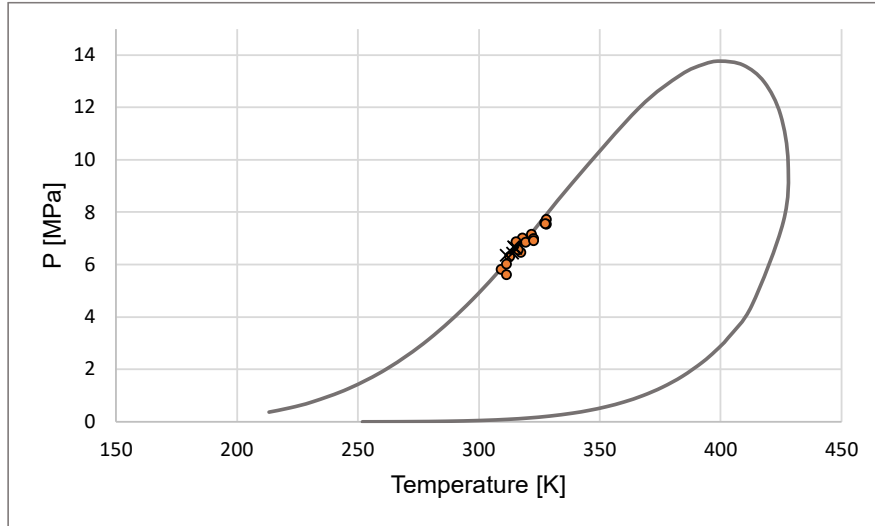

Figure 20. P-T diagram for the SRK model (non-temperature dependant).

$x\_CO_2 = 0.7491$; $x\_acet = 0.1285$; $x\_isoprop = 0.1224$. BIPs CO_2/Acetone: 0.0352; CO_2/Isopropanol: 0.0638; Isopropanol/Acetone: -0.0178
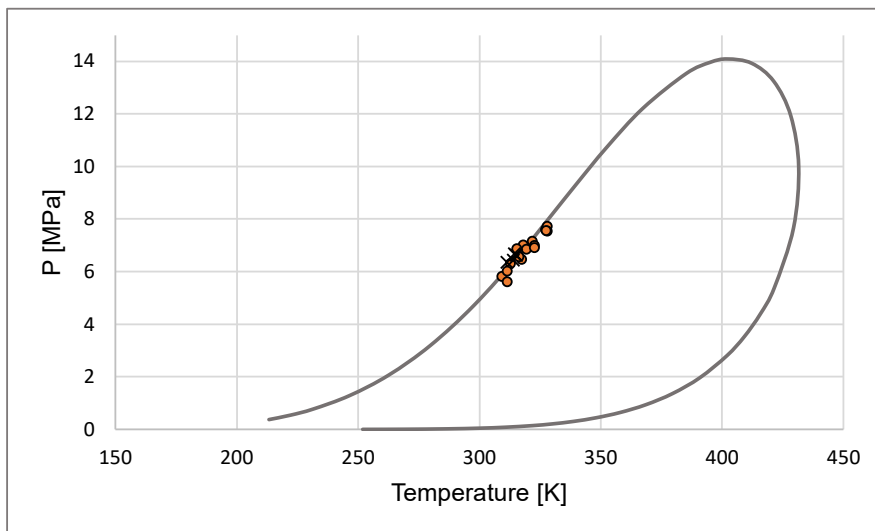
Figure 21. P-T diagram for the SRK model (temperature dependant).

$x\_CO_2 = 0.7491$; $x\_acet = 0.1285$; $x\_isoprop = 0.1224$

Both diagrams fit the points well for the stated composition. However, when the temperature is higher, the use of temperature-dependent parameters varies its maximum.

Plotting the estimated pressure data in the regression against the measured pressure, the fit appears to be correct, in the sense that there is not a large set of over- or underestimated data. It is intuitive how this (still acceptable) deviation takes place when the pressures are higher, approximately above 10 MPa, which was when the biggest measurement problems were found due to the lack of opacity in the cell. Comparing the fit between the PR model (Figure 22) and the SRK model (Figure 23), where the circles show the opacity points and the crosses show the redissolution points, the regressions do not show considerable deviations in the central part of the data, i.e. from pressures of about 5 MPa to about 85 MPa. It is at pressures above the latter that larger discrepancies are observed. Visually, it appears that for the SRK model the data for the estimated pressure are further away from the regression than for the PR model.
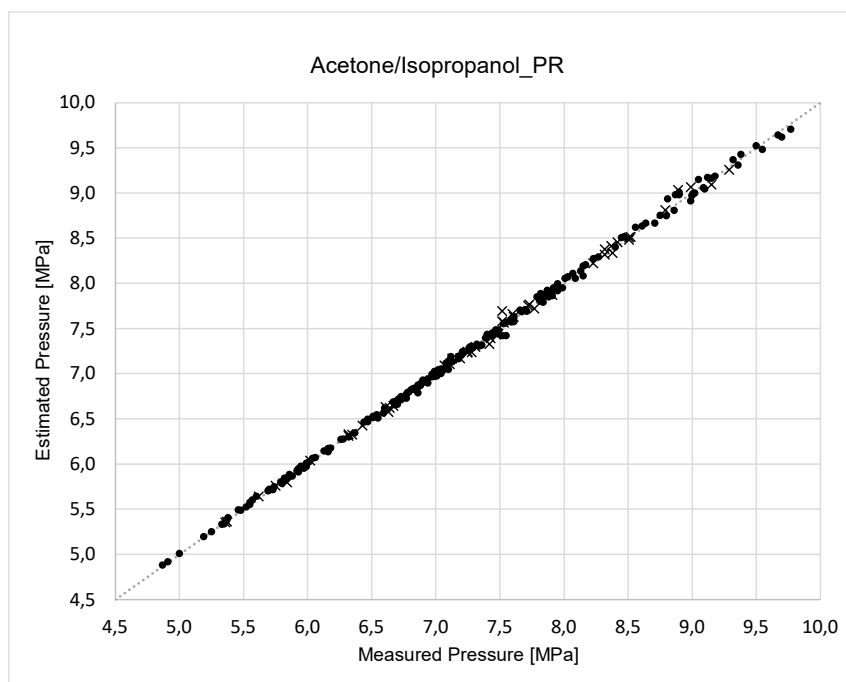
Figure 22. Estimated pressure vs measured pressure for the PR model.
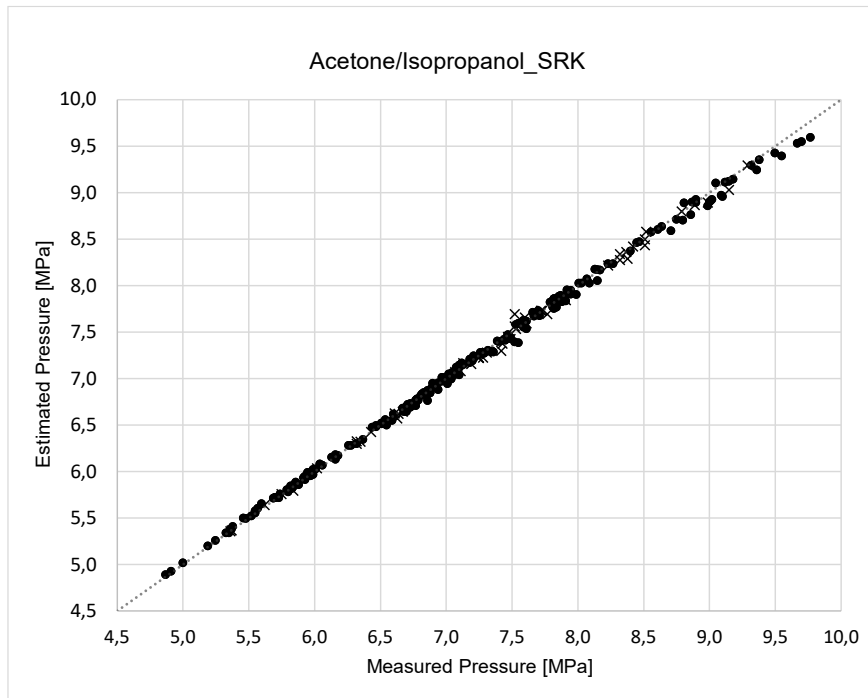
Figure 23. Estimated pressure vs measured pressure for the SRK model.

Similarly, the same regressions can be plotted for temperature (Figure 24 and Figure 25). In this case, the difference between the estimated and measured values is greater. The data are more dispersed with respect to the fit. If both thermodynamic models are compared, it is observed that at high temperatures (320-330 K), the SRK model overestimates the data with respect to the PR model.
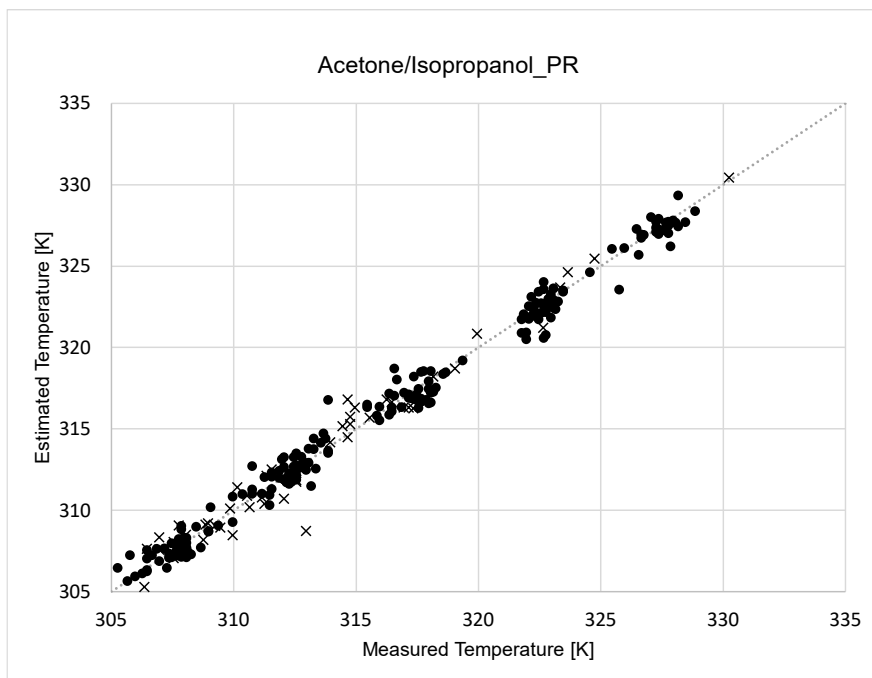
Figure 24. Estimated temperature vs measured temperature for the PR model.
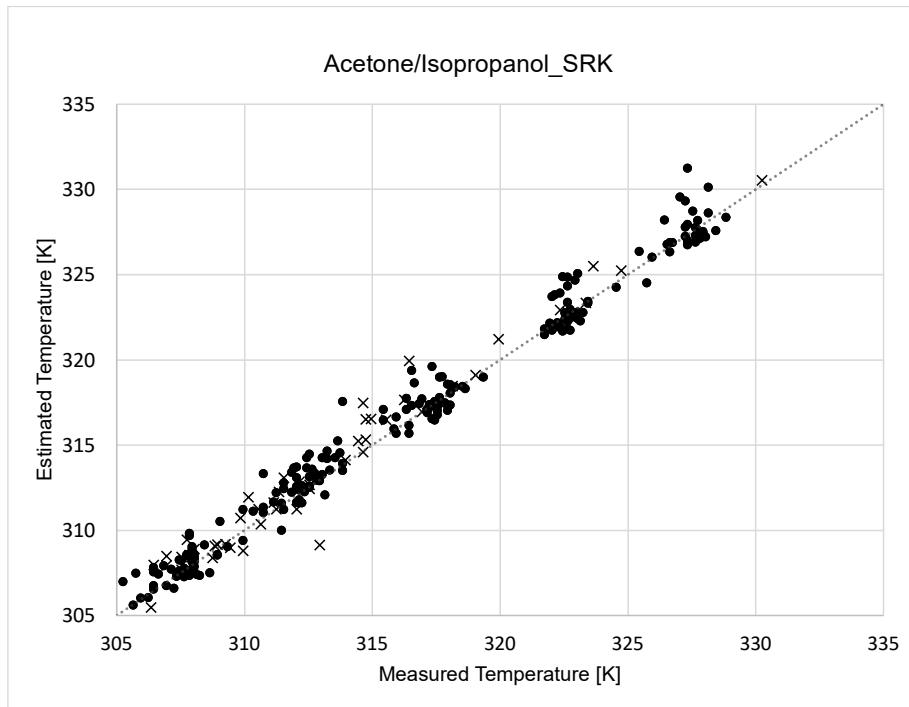
Figure 25. Estimated temperature vs measured temperature for the SRK model.

The larger deviance in the estimation of temperature compared to that of pressure may be explained by, for example the lower accuracy of temperature-measurements. However, both studied thermodynamic models proved to be suitable to describe the behaviour of the studied ternary mixture in the composition range of x_{CO_2} : $(0.7; 0.99)$; $x_{acetone}$: $(0.003; 0.24)$; x_{iPrOH} : $(0.001; 0.14)$, and in the pressure and temperature ranges of 5 and 14 MPa and 308.15-328.15 K, respectively.

5. Summary

The aim of this work is to investigate the phase behaviour of a system consisting of CO_2 + acetone + isopropanol. This is a ternary mixture for which no bibliographical references were found, although there were previous works on binary systems of CO_2 and acetone/isopropanol. For its analysis, a synthetic method with phase transition is used in order to obtain the cloud point pressures at varied compositions and temperatures. Subsequently, thermodynamic modelling is carried out using the Peng-Robinson (PR) and Soave-Redlich-Kwong (SRK) equations of state.

The study of the data for the three acetone/isopropanol volumetric ratios applied (1:1, 3:1 and 5:1) shows that the relation between pressure and temperature at a given composition for all of them has a linear upward trend. The greatest scatter in the data was observed for a 3:1 ratio while a greater homogeneity was seen for the 1:1 fraction. No substantial changes in pressures were observed between the different acetone to isopropanol ratios. Analysing the surface plots, it can be seen that the linear trend based on composition is modified when the mixture is close its the critical point, where a quadratic fit seems to be more appropriate.

With reference to the thermodynamic analysis, firstly, it was seen how the addition of points with compositions close to the critical point provided errors in the simulation, so filtering of the data was necessary. Subsequently, the three ratios studied were analysed globally and the opacity and redissolution data were also included together. On the other hand, the suitability of using the Peng-Robinson and Soave-Redlich-Kwong models to analyse the behaviour of the ternary mixture was investigated. This process was developed in two steps, depending on whether the temperature dependence was added to the binary interaction parameter. It was found for both models that the fit with the temperature dependence was more appropriate with the second k_{ij} term being negligible. A comparison of the PR and SRK models shows that the root mean square error obtained for PR is lower, which is also observable when the estimated pressure is plotted against the measured pressure. It was seen that when the pressure is high and higher than about 85 MPa, the deviation between the values increases. A similar thing happens with the temperature regression, where at temperatures above 320 K the PR model is observed to fit the data better. The deviation in the temperature regression is larger than for the pressure case, which may be due to a lower precision in the temperature measurement.

Based on this, the binary parameter values obtained for the best fit model (PR) were approximately (varies with temperature) -0.01 for the CO_2/acetone pair compared to -0.03 in the literature. For CO_2/isopropanol it was approximately -0.1 which is different from the 0.128 reported in the literature. For the acetone/isopropanol pair the approximate value is -0.44. No data were found in the literature with the same mixing rule for this pair.

In view of future work, it may be of interest to complement the study to confirm the reliability of the data. To this end, the use of other equilibrium measurement models, the variation of the proportions of acetone and isopropanol or the use of other thermodynamic models in the modelling may be proposals that could help. It would also be useful to see whether the binary parameters obtained here could be applicable to binary systems or to re-fit the literature binary parameters that use a different mixing rule and combine it for this ternary mixture.

6. Literature bibliography

AIDA, T., AIZAWA, T., KANAKUBO, M. and NANJO, H., 2010. Dependence of volume expansion on alkyl chain length and the existence of branched methyl group of CO2-expanded ketone systems at 40°C. *The Journal of Supercritical Fluids*, vol. 55, no. 1, pp. 71-76. ISSN 08968446. DOI 10.1016/j.supflu.2010.05.025.

ANASTAS, P. and EGHBALI, N., 2010. Green Chemistry: Principles and Practice. *Chem. Soc. Rev.*, vol. 39, no. 1, pp. 301-312. ISSN 0306-0012, 1460-4744. DOI 10.1039/B918763B.

BAMBERGER, A. and MAURER, G., 2000. High-pressure (vapour + liquid) equilibria in (carbon dioxide+ acetone or 2-propanol) at temperatures from 293 K to 333 K. *The Journal of Chemical Thermodynamics*, vol. 32, no. 5, pp. 685-700. ISSN 00219614. DOI 10.1006/jcht.1999.0641.

BOGEL-ŁUKASIK, E., SANTOS, S., BOGEL-ŁUKASIK, R. and NUNES DA PONTE, M., 2010. Selectivity enhancement in the catalytic heterogeneous hydrogenation of limonene in supercritical carbon dioxide by an ionic liquid. *The Journal of Supercritical Fluids*, vol. 54, no. 2, pp. 210-217. ISSN 08968446. DOI 10.1016/j.supflu.2010.04.011.

BOYÈRE, C., JÉRÔME, C. and DEBUIGNE, A., 2014. Input of supercritical carbon dioxide to polymer synthesis: An overview. *European Polymer Journal*, vol. 61, pp. 45-63. ISSN 00143057. DOI 10.1016/j.eurpolymj.2014.07.019.

BRAGA, A.J.O., TAVARES, F.W. and NDIAYE, P.M., 2021. A new high-pressure cell for equilibrium measurements of systems with fluid and solid phases. *The Journal of Supercritical Fluids*, vol. 179, pp. 105420. ISSN 08968446. DOI 10.1016/j.supflu.2021.105420.

BRANDT, L., ELIZALDE-SOLIS, O., GALICIA-LUNA, L.A. and GMEHLING, J., 2010. Solubility and density measurements of palmitic acid in supercritical carbon dioxide+alcohol mixtures. *Fluid Phase Equilibria*, vol. 289, n. 1, pp. 72-79. ISSN 03783812. DOI 10.1016/j.fluid.2009.11.007.

BRUN, K., FRIEDMAN, P. and DENNIS, R., 2017. Fundamentals and Applications of Supercritical Carbon Dioxide (SCO_2) Based Power Cycles. *Elsevier Ltd*, pp. 464. ISSN 978-0-08-100805-8.

BRUNNER, G., 2010. Applications of Supercritical Fluids. *Annual Review of Chemical and Biomolecular Engineering*, vol. 1, no. 1, pp. 321-342. ISSN 1947-5438, 1947-5446. DOI 10.1146/annurev-chembioeng-073009-101311.

CRESPI, F., GAVAGNIN, G., SÁNCHEZ, D. and MARTÍNEZ, G.S., 2017. Supercritical carbon dioxide cycles for power generation: A review. *Applied Energy*, vol. 195, pp. 152-183. ISSN 03062619. DOI 10.1016/j.apenergy.2017.02.048.

DELL'ERA, C., ZAYTSEVA, A., UUSI-KYYNY, P., POKKI, J.-P., PAKKANEN, M. and AITTAMAA, J., 2007. Vapour–liquid equilibrium for the systems

butane+methanol, +2-propanol, +1-butanol, +2-butanol, +2-methyl-2-propanol at 364.5K. *Fluid Phase Equilibria*, vol. 254, no. 1-2, pp. 49-59. ISSN 03783812. DOI 10.1016/j.fluid.2007.02.028.

DJAS, M. and HENCZKA, M., 2018. Reactive extraction of carboxylic acids using organic solvents and supercritical fluids: A review. *Separation and Purification Technology*, vol. 201, pp. 106-119. ISSN 13835866. DOI 10.1016/j.seppur.2018.02.010.

ERKEY, C., 2000. Supercritical carbon dioxide extraction of metals from aqueous solutions: a review. *The Journal of Supercritical Fluids*, vol. 17, no. 3, pp. 259-287. ISSN 08968446. DOI 10.1016/S0896-8446(99)00047-9.

ERKEY, C., 2011. Homogeneous Catalysis in Supercritical Fluids. *Supercritical Fluid Science and Technology* [en línea]. S.l.: Elsevier, pp. 161-209. [Accessed: 15 December 2021]. ISBN 978-0-08-045329-3. Available in: https://linkinghub.elsevier.com/retrieve/pii/B978008045329300007X.

FONSECA, J.M.S., DOHRN, R. and PEPER, S., 2011. High-pressure fluid-phase equilibria: Experimental methods and systems investigated (2005–2008). *Fluid Phase Equilibria*, vol. 300, no. 1-2, pp. 1-69. ISSN 03783812. DOI 10.1016/j.fluid.2010.09.017.

FONSECA, J.M.S. and VON SOLMS, N., 2012. Development and testing of a new apparatus for the measurement of high-pressure low-temperature phase equilibria. *Fluid Phase Equilibria*, vol. 329, pp. 55-62. ISSN 03783812. DOI 10.1016/j.fluid.2012.05.024.

GALICIA-LUNA, L.A. and ELIZALDE-SOLIS, O., 2010. New analytic apparatus for experimental determination of vapor–liquid equilibria and saturation densities. *Fluid Phase Equilibria*, vol. 296, no. 1, pp. 46-52. ISSN 03783812. DOI 10.1016/j.fluid.2010.03.004.

GANG, Z., HUAN-FENG, J. and MING-CAI, C., 2003. Chemical reactions in supercritical carbon dioxide. , pp. 8.

GRANDELLI, H.E., HASSLER, J.C., WHITTINGTON, A. and KIRAN, E., 2012. Melting point depression of Piroxicam in carbon dioxide+co-solvent mixtures and inclusion complex formation with β-cyclodextrin. *The Journal of Supercritical Fluids*, vol. 71, pp. 19-25. ISSN 08968446. DOI 10.1016/j.supflu.2012.07.001.

HAN, F.Y., KOMIYAMA, M., UEMURA, Y. and RABAT, N.E., 2020. Catalytic alcohothermal liquefaction of wet microalgae with supercritical methanol. *The Journal of Supercritical Fluids*, vol. 157, pp. 104704. ISSN 08968446. DOI 10.1016/j.supflu.2019.104704.

HRNČIČ, M.K., KRAVANJA, G. and KNEZ, Ž., 2016. Hydrothermal treatment of biomass for energy and chemicals. *Energy*, vol. 116, pp. 1312-1322. ISSN 03605442. DOI 10.1016/j.energy.2016.06.148.

IKARIYA, T. and KAYAKI, Y., 2000. Supercritical fluids as reaction media for molecular catalysis. , vol. 4, pp. 39-50. DOI 10.1023/A:1019032004130.

IMAI, M., OTO, Y., NITTA, S., TAKEYA, S. and OHMURA, R., 2012. Phase equilibrium for structure II clathrate hydrates formed with (fluoromethane+propan-2-ol, 2-methyl-2-propanol, or 2-propanone). *The Journal of Chemical Thermodynamics*, vol. 47, pp. 17-20. ISSN 00219614. DOI 10.1016/j.jct.2011.09.020.

KESHTKARI, S., HAGHBAKHSH, R., RAEISSI, S., FLORUSSE, L. and PETERS, C.J., 2013. Vapor–liquid equilibria of isopropyl alcohol+propylene at high pressures: Experimental measurement and modeling with the CPA EoS. *The Journal of Supercritical Fluids*, vol. 84, pp. 182-189. ISSN 08968446. DOI 10.1016/j.supflu.2013.09.016.

KHOIROH, I. and LEE, M.-J., 2011. Isothermal Vapor−Liquid Equilibrium for Binary Mixtures of Polyoxyethylene 4-Octylphenyl Ether with Methanol, Ethanol, or Propan-2-ol. *Journal of Chemical & Engineering Data*, vol. 56, no. 4, pp. 1178-1184. ISSN 0021-9568, 1520-5134. DOI 10.1021/je101096p.

KIM, S.A., LIM, J.S. and KANG, J.W., 2010. Isothermal Vapor−Liquid Equilibria for the Binary System of Carbon Dioxide (CO_2) + 1,1,1,2,3,3,3-Heptafluoropropane (R-227ea). *Journal of Chemical & Engineering Data*, vol. 55, no. 11, pp. 4999-5003. ISSN 0021-9568, 1520-5134. DOI 10.1021/je100583z.

KIRAN, E., DEBENEDETTI, P.G. and PETERS, C.J., 2000. *Supercritical Fluids* [online]. Dordrecht: Springer Netherlands. [Accessed: 26 October 2021]. ISBN 978-0-7923-6236-4. Available in: http://link.springer.com/10.1007/978-94-011-3929-8.

KIRAN, E. and SENGERS, J.M.H.L., 1994. *Supercritical Fluids* [online]. Dordrecht: Springer Netherlands. [Accessed: 3 November 2021]. ISBN 978-90-481-4427-3. Available in: http://link.springer.com/10.1007/978-94-015-8295-7.

KNEZ, Ž., MARKOČIČ, E., LEITGEB, M., PRIMOŽIČ, M., KNEZ HRNČIČ, M. and ŠKERGET, M., 2014. Industrial applications of supercritical fluids: A review. *Energy*, vol. 77, pp. 235-243. ISSN 03605442. DOI 10.1016/j.energy.2014.07.044.

KNEZ, Ž., ŠKERGET, M. and KNEZHRNČIČ, M., 2013. Principles of supercritical fluid extraction and applications in the food, beverage and nutraceutical industries. *Separation, Extraction and Concentration Processes in the Food, Beverage and Nutraceutical Industries* [online]. S.l.: Elsevier, pp. 3-38. [Accessed: 22 November 2021]. ISBN 978-1-84569-645-0. Available in: https://linkinghub.elsevier.com/retrieve/pii/B9781845696450500013.

KONG, X., LIU, C., XU, W., HAN, Y., FAN, Y., LEI, M., LI, M. and XIAO, R., 2021. Catalytic hydroprocessing of stubborn lignin in supercritical methanol with Cu/CuMgAlOx catalyst. *Fuel Processing Technology*, vol. 218, pp. 106869. ISSN 03783820. DOI 10.1016/j.fuproc.2021.106869.

KROON, M.C., FLORUSSE, L.J., KÜHNE, E., WITKAMP, G.-J. and PETERS, C.J., 2010. Achievement of a Homogeneous Phase in Ternary Ionic Liquid/Carbon Dioxide/Organic Systems. *Industrial & Engineering Chemistry Research*, vol.

49, no. 7, pp. 3474-3478. ISSN 0888-5885, 1520-5045. DOI 10.1021/ie901405p.

LATSKY, C., CORDEIRO, B. and SCHWARZ, C.E., 2020. High pressure bubble- and dew-point data for systems containing CO2 with 1-decanol and n-hexadecane. *Fluid Phase Equilibria*, vol. 521, pp. 112702. ISSN 03783812. DOI 10.1016/j.fluid.2020.112702.

LAZZARONI, M.J., BUSH, D., ECKERT, C.A. and GLÄSER, R., 2006. High-pressure vapor–liquid equilibria of argon+carbon dioxide+2-propanol. *The Journal of Supercritical Fluids*, vol. 37, no. 2, pp. 135-141. ISSN 08968446. DOI 10.1016/j.supflu.2005.10.002.

LEI, Z., QI, X., ZHU, J., LI, Q. and CHEN, B., 2012. Solubility of CO2 in Acetone, 1-Butyl-3-methylimidazolium Tetrafluoroborate, and Their Mixtures. *Journal of Chemical & Engineering Data*, vol. 57, no. 12, pp. 3458-3466. ISSN 0021-9568, 1520-5134. DOI 10.1021/je300611q.

LI, K. and XU, Z., 2019. A review of current progress of supercritical fluid technologies for e-waste treatment. *Journal of Cleaner Production*, vol. 227, pp. 794-809. ISSN 09596526. DOI 10.1016/j.jclepro.2019.04.104.

MAEKAWA, T., 2011. Equilibrium conditions of clathrate hydrates formed from carbon dioxide and aqueous acetone solutions. *Fluid Phase Equilibria*, vol. 303, no. 1, pp. 76-79. ISSN 03783812. DOI 10.1016/j.fluid.2011.01.011.

MALHOTRA, R. and WOOLF, L.A., 1991. Thermodynamic properties of propanone (acetone) at temperatures from 278 K to 323 K and pressures up to 400 MPa. *The Journal of Chemical Thermodynamics*, vol. 23, no. 9, pp. 867-876. ISSN 00219614. DOI 10.1016/S0021-9614(05)80282-4.

MATSUDA, T., 2013. Recent progress in biocatalysis using supercritical carbon dioxide. *Journal of Bioscience and Bioengineering*, vol. 115, no. 3, pp. 233-241. ISSN 13891723. DOI 10.1016/j.jbiosc.2012.10.002.

MELHEM, G.A., SAINI, R. and GOODWIN, B.M., 1989. A modified Peng-Robinson equation of state. *Fluid Phase Equilibria*, vol. 47, no. 2, pp. 189-237. ISSN 0378-3812. DOI 10.1016/0378-3812(89)80176-1.

NIKOLAI, P., RABIYAT, B., ASLAN, A. and ILMUTDIN, A., 2019. Supercritical CO2: Properties and Technological Applications - A Review. *Journal of Thermal Science*, vol. 28, no. 3, pp. 394-430. ISSN 1003-2169, 1993-033X. DOI 10.1007/s11630-019-1118-4.

NIST. [online], 2021. [Accessed: 27 November 2021]. Available in: https://webbook.nist.gov/chemistry/fluid/.

NOVITSKIY, A.A., PÉREZ, E., WU, W., KE, J. and POLIAKOFF, M., 2009. A New Continuous Method for Performing Rapid Phase Equilibrium Measurements on Binary Mixtures Containing CO $_2$ or H $_2$ O at High Pressures and Temperatures. *Journal of Chemical & Engineering Data*, vol. 54, no. 5, pp. 1580-1584. ISSN 0021-9568, 1520-5134. DOI 10.1021/je800923q.

PASANEN, M., ZAYTSEVA, A., UUSI-KYYNY, P., POKKI, J.-P., PAKKANEN, M. and AITTAMAA, J., 2006. Vapor Liquid Equilibrium for Six Binary Systems of C_4-Hydrocarbons + 2-Propanone. *Journal of Chemical & Engineering Data*, vol. 51, no. 2, pp. 554-561. ISSN 0021-9568, 1520-5134. DOI 10.1021/je050403k.

PENG, D.-Y. and ROBINSON, D.B., 1976. A New Two-Constant Equation of State. *Industrial & Engineering Chemistry Fundamentals*, vol. 15, no. 1, pp. 59-64. ISSN 0196-4313, 1541-4833. DOI 10.1021/i160057a011.

PEPER, S., FONSECA, J.M.S. and DOHRN, R., 2019. High-pressure fluid-phase equilibria: Trends, recent developments, and systems investigated (2009–2012). *Fluid Phase Equilibria*, vol. 484, pp. 126-224. ISSN 03783812. DOI 10.1016/j.fluid.2018.10.007.

POLING, B.E., PRAUSNITZ, J.M. and O´CONNELL, J.P., 2001. The Properties of Gases and Liquids. Fifth Edition. *McGraw Hill Professional*, pp. 708. ISSN 9780070116825.

RADOSZ, M., 1986. Vapor-liquid equilibrium for 2-propanol and carbon dioxide. *Journal of Chemical & Engineering Data*, vol. 31, no. 1, pp. 43-45. ISSN 0021-9568, 1520-5134. DOI 10.1021/je00043a014.

RAMSEY, E., SUN, Q., ZHANG, Z., ZHANG, C. and GOU, W., 2009. Mini-Review: Green sustainable processes using supercritical fluid carbon dioxide. *Journal of Environmental Sciences*, vol. 21, no. 6, pp. 720-726. ISSN 10010742. DOI 10.1016/S1001-0742(08)62330-X.

SHAFI, S., RASHEED, T., NAZ, R., MAJEED, S. and BILAL, M., 2021. Supercritical CO2 drying of pure silica aerogels: effect of drying time on textural properties of nanoporous silica aerogels. *Journal of Sol-Gel Science and Technology*, vol. 98, no. 3, pp. 478-486. ISSN 0928-0707, 1573-4846. DOI 10.1007/s10971-021-05530-0.

SOAVE, G., 1971. *Equilibrium constants from a modified Redkh-Kwong equation of state*. 1971. S.l.: s.n.

SPAN, R. and WAGNER, W., 1996. A New Equation of State for Carbon Dioxide Covering the Fluid Region from the Triple-Point Temperature to 1100 K at Pressures up to 800 MPa. *Journal of Physical and Chemical Reference Data*, vol. 25, no. 6, pp. 1509-1596. ISSN 0047-2689, 1529-7845. DOI 10.1063/1.555991.

SUZUKI, T., TSUGE, N. and NAGAHAMA, K., 1991. Solubilities of ethanol, l-propanol, 2-propanol and l- butanol in supercritical carbon dioxide at 313 K and 333 K. , pp. 14.

TSAI, W.-C. and WANG, Y., 2019. Progress of supercritical fluid technology in polymerization and its applications in biomedical engineering. *Progress in Polymer Science*, vol. 98, pp. 101161. ISSN 00796700. DOI 10.1016/j.progpolymsci.2019.101161.

ULANOVA, T., TUMA, D. and MAURER, G., 2009. Salt Effect on the High-Pressure Multiphase Behavior of the Ternary System (Ethene + Water + 2-Propanol). *Journal of Chemical & Engineering Data*, vol. 54, no. 5, pp. 1417-1420. ISSN 0021-9568, 1520-5134. DOI 10.1021/je800401g.

WANG, W., RAO, L., WU, X., WANG, Y., ZHAO, L. and LIAO, X., 2021. Supercritical Carbon Dioxide Applications in Food Processing. *Food Engineering Reviews*, vol. 13, no. 3, pp. 570-591. ISSN 1866-7910, 1866-7929. DOI 10.1007/s12393-020-09270-9.

WHITE, M.T., BIANCHI, G., CHAI, L., TASSOU, S.A. and SAYMA, A.I., 2021. Review of supercritical CO 2 technologies and systems for power generation. *Applied Thermal Engineering*, vol. 185, pp. 116447. ISSN 13594311. DOI 10.1016/j.applthermaleng.2020.116447.

WU, J., PAN, Q. and REMPEL, G.L., 2004. Pressure−Density−Temperature Behavior of CO 2 /Acetone, CO 2 /Toluene, and CO 2 /Monochlorobenzene Mixtures in the Near-Critical Region. *Journal of Chemical & Engineering Data*, vol. 49, no. 4, pp. 976-979. ISSN 0021-9568, 1520-5134. DOI 10.1021/je0342771.

XIE, G., XU, X., LEI, X., LI, Z., LI, Y. and SUNDEN, B., 2021. Heat transfer behaviors of some supercritical fluids: A review. *Chinese Journal of Aeronautics*, pp. S1000936120305835. ISSN 10009361. DOI 10.1016/j.cja.2020.12.022.

XU, J., PENG, Z., RONG, S., JIN, H., GUO, L., ZHANG, X. and ZHOU, T., 2021. Model-based thermodynamic analysis of supercritical water gasification of oil-containing wastewater. *Fuel*, vol. 306, pp. 121767. ISSN 00162361. DOI 10.1016/j.fuel.2021.121767.

YAGINUMA, R., NAKAJIMA, T., TANAKA, H. and KATO, M., 1997. Densities of Carbon Dioxide + 2-Propanol at 313.15 K and Pressures to 9.8 MPa. *Journal of Chemical & Engineering Data*, vol. 42, no. 4, pp. 814-816. ISSN 0021-9568, 1520-5134. DOI 10.1021/je9700028.

YEO, S.-D. and KIRAN, E., 2005. Formation of polymer particles with supercritical fluids: A review. *The Journal of Supercritical Fluids*, vol. 34, no. 3, pp. 287-308. ISSN 08968446. DOI 10.1016/j.supflu.2004.10.006.

7. Appendix

7.1. Molar density of CO_2 in the applied temperature range.

Table 15. Molar densities of CO_2 from NIST.

T^a (ºC)	density (mol/L)
26	20.667
25.9	20.678
25.8	20.688
25.7	20.699
25.6	20.721
25.4	20.731
25.3	20.742
25.2	20.752
25.1	20.763
25	20.773
24.9	20.784
24.8	20.794
24.7	20.805
24.6	20.816
24.5	20.826
24.4	20.837
24.3	20.847
24.2	20.858
24.1	20.868
24	20.879
23.9	20.889
23.8	20.900

7.2. Laboratory measurements. Opacity Points.

Table 16. Laboratory raw data. Opacity points. Bold Type: Data included in Aspen.

	1:1 Acet/Isop.			3:1 Acet/Isop.			5:1 Acet/Isop.	
x_CO_2	T[K]	P[MPa]	x_CO_2	T[K]	P[MPa]	x_CO_2	T[K]	P[MPa]
0.7118	**305.65**	**5.25**	**0.7668**	**307.75**	**5.88**	**0.7129**	**307.65**	**4.91**
0.7118	**306.95**	**5.33**	**0.7668**	**308.15**	**5.38**	**0.7129**	**307.15**	**5.35**
0.7118	**307.65**	**5.37**	**0.7668**	**308.05**	**5.83**	**0.7129**	**308.05**	**4.87**
0.7118	**312.15**	**5.69**	**0.7668**	**306.45**	**5.52**	**0.7129**	**308.95**	**5**
0.7118	**312.05**	**5.74**	**0.7668**	**312.25**	**5.82**	**0.7129**	**310.75**	**5.73**
0.7118	**312.15**	**5.7**	**0.7668**	**311.85**	**6.18**	**0.7129**	**312.75**	**5.93**
0.7118	**316.45**	**5.99**	**0.7668**	**312.35**	**6.06**	**0.7129**	**313.85**	**5.48**
0.7118	**317.95**	**6.04**	**0.7668**	**312.15**	**5.93**	**0.7129**	**317.15**	**5.92**

0.7118	**317.45**	**5.95**	**0.7668**	**316.55**	**6.85**	**0.7129**	**318.65**	**5.92**
0.7118	**322.85**	**6.92**	**0.7668**	**316.55**	**7.52**	**0.7129**	**317.15**	**5.85**
0.7118	**322.55**	**6.91**	**0.7668**	**315.85**	**6.51**	**0.7129**	**322.35**	**6.13**
0.7118	**321.85**	**6.86**	**0.7668**	**315.95**	**6.75**	**0.7129**	**322.95**	**6.26**
0.7118	**324.55**	**7.05**	**0.7668**	**318.55**	**6.71**	**0.7129**	**322.25**	**6.47**
0.7118	**327.75**	**7.11**	**0.7668**	**322.15**	**7.04**	**0.7129**	**322.35**	**6.16**
0.7118	**326.65**	**7.26**	**0.7668**	**323.25**	**7.02**	**0.7129**	**327.25**	**7.04**
0.7491	**308.45**	**5.97**	**0.7668**	**322.05**	**6.99**	**0.7129**	**325.95**	**6.97**
0.7491	**308.65**	**5.46**	**0.7668**	**325.45**	**7.95**	**0.7129**	**326.65**	**7.18**
0.7491	**306.65**	**5.8**	**0.7668**	**327.75**	**7.6**	**0.7499**	**307.35**	**5.36**
0.7491	**305.95**	**5.55**	**0.7668**	**327.75**	**7.7**	**0.7499**	**306.25**	**5.19**
0.7491	**309.35**	**5.79**	**0.7668**	**327.65**	**7.83**	**0.7499**	**308.95**	**5.36**
0.7491	**311.45**	**5.6**	**0.7927**	**308.25**	**5.57**	**0.7499**	**311.25**	**6.16**
0.7491	**312.85**	**6.28**	**0.7927**	**307.95**	**5.7**	**0.7499**	**310.35**	**5.99**
0.7491	**311.55**	**6.01**	**0.7927**	**307.25**	**5.55**	**0.7499**	**310.75**	**5.84**
0.7491	**317.35**	**6.44**	**0.7927**	**309.95**	**5.86**	**0.7499**	**313.75**	**6.37**
0.7491	**318.05**	**6.99**	**0.7927**	**311.55**	**6.59**	**0.7499**	**313.25**	**6.55**
0.7491	**316.45**	**6.54**	**0.7927**	**311.95**	**6.77**	**0.7499**	**313.55**	**6.32**
0.7491	**315.45**	**6.85**	**0.7927**	**310.75**	**6.86**	**0.7499**	**323.05**	**6.82**
0.7491	**319.35**	**6.83**	**0.7927**	**313.65**	**6.94**	**0.7499**	**323.45**	**7.02**
0.7491	**321.75**	**7.13**	**0.7927**	**315.95**	**6.6**	**0.7499**	**323.45**	**6.94**
0.7491	**322.65**	**6.97**	**0.7927**	**317.65**	**7.35**	**0.7499**	**326.75**	**7.47**
0.7491	**322.75**	**6.9**	**0.7927**	**317.15**	**6.81**	**0.7499**	**327.75**	**7.39**
0.7491	**327.35**	**7.59**	**0.7927**	**317.75**	**7.34**	**0.7499**	**327.95**	**7.18**
0.7491	**327.95**	**7.7**	**0.7927**	**323.15**	**7.1**	**0.8961**	**306.85**	**6.68**
0.7491	**328.05**	**7.53**	**0.7927**	**322.45**	**7.08**	**0.8961**	**307.65**	**6.51**
0.7491	**327.65**	**7.55**	**0.7927**	**313.85**	**7.55**	**0.8961**	**307.85**	**6.47**
0.8930	**307.85**	**7.01**	**0.7927**	**323.05**	**7.21**	**0.8961**	**312.55**	**7.29**
0.8930	**307.95**	**6.88**	**0.7927**	**327.65**	**7.86**	**0.8961**	**312.25**	**7.2**
0.8930	**307.75**	**6.79**	**0.7927**	**328.85**	**7.92**	**0.8961**	**313.05**	**7.27**
0.8930	**312.45**	**7.49**	**0.7927**	**328.45**	**7.66**	**0.8961**	**316.65**	**8.15**
0.8930	**313.35**	**7.4**	**0.7927**	**327.35**	**7.84**	**0.8961**	**315.45**	**7.91**
0.8930	**312.45**	**7.61**	**0.9052**	**306.45**	**6.73**	**0.8961**	**316.95**	**7.89**
0.8930	**318.15**	**8.03**	**0.9052**	**305.25**	**6.7**	**0.8961**	**322.15**	**8.8**
0.8930	**317.65**	**7.95**	**0.9052**	**307.95**	**6.88**	**0.8961**	**322.65**	**8.99**
0.8930	**316.85**	**7.94**	**0.9052**	**308.05**	**6.73**	**0.8961**	**322.65**	**8.86**
0.8930	**322.45**	**9.1**	**0.9052**	**312.15**	**7.27**	**0.8961**	**328.15**	**9.7**
0.8930	**323.05**	**9.09**	**0.9052**	**312.35**	**7.26**	**0.8961**	**326.45**	**9.36**
0.8930	**322.95**	**9.01**	**0.9052**	**312.55**	**7.27**	**0.8961**	**327.35**	**9.18**
0.8930	**327.55**	**9.5**	**0.9052**	**313.15**	**7.12**	**0.8961**	**327.25**	**9.15**
0.8930	**327.25**	**9.67**	**0.9052**	**317.85**	**7.87**	**0.9100**	**307.65**	**6.7**
0.8930	**327.05**	**9.77**	**0.9052**	**318.05**	**7.82**	**0.9100**	**308.05**	**6.77**
0.9351	**308.05**	**7.09**	**0.9052**	**317.55**	**7.79**	**0.9100**	**307.95**	**6.67**
0.9351	**308.05**	**6.99**	**0.9052**	**317.95**	**7.82**	**0.9100**	**312.05**	**7.45**
0.9351	**307.85**	**7.36**	**0.9052**	**322.95**	**8.56**	**0.9100**	**313.25**	**7.59**
0.9351	**311.85**	**7.82**	**0.9052**	**321.75**	**8.47**	**0.9100**	**313.85**	**7.47**

Table 16. Laboratory raw data. Opacity points. Bold Type: Data included in Aspen (3/5)

0.9351	**312.55**	**7.99**	**0.9052**	**321.95**	**8.45**	**0.9100**	**316.35**	**8.09**
0.9351	**312.65**	**7.81**	**0.9052**	**326.55**	**9.12**	**0.9100**	**317.45**	**7.94**
0.9351	**316.35**	**8.27**	**0.9052**	**328.15**	**9.38**	**0.9100**	**317.25**	**7.92**
0.9351	**317.35**	**8.71**	**0.9052**	**327.85**	**9.05**	**0.9100**	**322.75**	**8.64**
0.9351	**317.55**	**8.13**	**0.9052**	**327.75**	**9.32**	**0.9100**	**322.65**	**8.75**
0.9351	**321.95**	**8.9**	**0.9181**	**306.45**	**6.68**	**0.9100**	**322.55**	**8.61**
0.9351	**322.65**	**8.87**	**0.9181**	**307.45**	**6.78**	0.9100	327.35	9.73
0.9351	**322.75**	**8.9**	**0.9181**	**307.95**	**6.86**	0.9100	327.65	9.56
0.9351	327.75	9.72	**0.9181**	**312.05**	**7.44**	**0.9100**	**327.35**	**9.55**
0.9351	328.05	9.61	**0.9181**	**311.45**	**7.28**	0.9100	327.85	9.99
0.9351	327.65	9.93	**0.9181**	**311.15**	**7.32**	**0.9368**	**306.45**	**7.04**
0.9444	306.85	7.3	**0.9181**	**317.65**	**8.01**	**0.9368**	**307.55**	**7.05**
0.9444	307.45	7.31	**0.9181**	**318.25**	**8.17**	**0.9368**	**307.45**	**7.06**
0.9444	**307.55**	**7.07**	**0.9181**	**317.65**	**8.07**	**0.9368**	**307.35**	**6.89**
0.9444	**311.15**	**7.61**	**0.9181**	**322.05**	**9**	**0.9368**	**307.95**	**7.01**
0.9444	**312.55**	**7.73**	**0.9181**	**322.35**	**9.02**	**0.9368**	**309.95**	**7.48**
0.9444	**311.25**	**7.53**	**0.9181**	**325.75**	**8.81**	**0.9368**	**312.05**	**7.84**
0.9444	**317.15**	**8.37**	0.9181	327.05	10.7	**0.9368**	**312.95**	**7.61**
0.9444	**319.05**	**8.79**	0.9181	327.05	10.32	**0.9368**	**313.05**	**7.88**
0.9444	**318.15**	**8.51**	0.9181	327.15	10.1	**0.9368**	**318.05**	**8.23**
0.9444	**322.35**	**8.99**	**0.9512**	**307.85**	**7.25**	**0.9368**	**317.95**	**8.4**
0.9444	**323.35**	**9.29**	**0.9512**	**307.55**	**7.25**	0.9368	316.55	7.99
0.9444	**322.65**	**8.89**	**0.9512**	**308.05**	**7.31**	**0.9368**	**317.55**	**8.15**
0.9444	326.65	9.48	**0.9512**	**306.95**	**7.19**	0.9368	322.55	9.23
0.9444	328.65	9.56	**0.9512**	**311.55**	**7.91**	0.9368	322.65	9.36
0.9444	328.65	9.48	**0.9512**	**312.55**	**7.72**	0.9368	322.75	9.09
0.9798	**306.35**	**7.13**	**0.9512**	**312.05**	**7.52**	0.9368	322.55	8.96
0.9798	307.45	7.13	**0.9512**	**310.15**	**7.77**	0.9368	326.75	10.14
0.9798	307.35	7.17	**0.9512**	**317.35**	**8.32**	0.9368	326.35	10.59
0.9798	307.15	7.24	**0.9512**	**314.75**	**8.38**	0.9368	327.55	10.36
0.9798	311.65	7.66	**0.9512**	**315.55**	**8.32**	0.9368	327.95	10.5
0.9798	311.75	7.66	**0.9512**	**316.25**	**8.51**	**0.9454**	**305.75**	**7.1**
0.9798	311.75	7.69	0.9512	320.15	9.22	0.9454	308.45	7.25
0.9798	**312.05**	**7.65**	0.9512	321.05	9.11	0.9454	305.95	7.05
0.9798	317.05	8.29	0.9512	322.15	9.42	0.9454	307.65	7.04
0.9798	317.05	8.29	0.9512	322.35	9.23	**0.9454**	**309.05**	**7.49**
0.9798	317.35	8.33	0.9512	327.95	9.92	0.9454	312.65	7.49
0.9798	317.25	8.28	0.9512	327.35	10.22	**0.9454**	**312.55**	**7.67**
0.9798	322.45	8.88	0.9512	327.65	9.78	**0.9454**	**311.55**	**7.71**
0.9798	322.85	8.82	0.9512	328.35	10.29	0.9454	317.45	8.45
0.9798	321.05	8.72	**0.9570**	**306.45**	**7.28**	0.9454	316.65	8.51
0.9798	322.85	9.01	**0.9570**	**307.75**	**7.49**	0.9454	317.65	8.65
0.9798	327.25	9.6	0.9570	307.85	7.42	0.9454	317.35	8.66
0.9798	327.85	9.63	0.9570	307.35	7.31	0.9454	321.55	9.36
0.9798	327.15	9.33	0.9570	311.05	7.78	0.9454	321.65	8.96
0.9798	328.25	9.47	**0.9570**	**312.15**	**7.89**	0.9454	321.95	9.19
0.9822	306.65	7.15	0.9570	310.65	7.83	0.9454	321.85	8.86

0.9822	307.75	7.16	0.9570	310.25	7.71	0.9454	327.65	10.52
0.9822	307.95	7.26	**0.9570**	**316.45**	**8.52**	0.9454	326.95	10.07
0.9822	307.15	7.21	**0.9570**	**316.95**	**8.42**	0.9454	327.75	10.04
0.9822	**309.95**	**7.6**	0.9570	316.45	8.67	0.9454	328.35	10.3
0.9822	**312.95**	**7.52**	0.9570	314.25	8.31	0.9759	306.05	7.13
0.9822	313.15	7.64	0.9570	320.15	9.42	0.9759	307.85	7.34
0.9822	313.65	7.85	0.9570	320.35	9.51	0.9759	307.45	7.33
0.9822	316.85	8.07	0.9570	320.75	9.47	0.9759	308.25	7.48
0.9822	317.85	8.27	0.9570	320.95	9.48	0.9759	310.65	7.84
0.9822	318.15	8.31	0.9570	325.55	10.18	0.9759	311.65	7.71
0.9822	317.85	8.41	0.9570	326.35	10.39	0.9759	313.05	7.86
0.9822	322.65	8.93	0.9570	325.75	10.18	0.9759	312.25	7.78
0.9822	322.75	9.05	0.9570	326.55	10.09	0.9759	316.25	8.35
0.9822	322.45	8.98	0.9775	307.65	7.13	0.9759	316.75	8.43
0.9822	322.55	8.89	0.9775	308.75	7.24	0.9759	316.95	8.56
0.9822	327.05	9.91	0.9775	308.95	7.3	0.9759	317.45	8.67
0.9822	327.55	9.75	0.9775	308.25	7.18	0.9759	322.55	9.56
0.9822	328.35	9.79	0.9775	312.25	7.62	0.9759	322.05	9.55
0.9822	328.05	9.89	0.9775	313.05	7.76	0.9759	322.45	9.63
0.9939	306.85	7.18	0.9775	312.15	7.79	0.9759	323.45	9.5
0.9939	305.75	7.12	0.9775	313.05	8.18	0.9759	327.15	10.27
0.9939	306.95	7.14	0.9775	315.75	8.21	0.9759	327.95	10.34
0.9939	306.25	7.09	0.9775	316.65	8.15	0.9759	327.45	10.41
0.9939	311.85	7.56	0.9775	317.25	8.39	0.9759	327.05	10.48
0.9939	311.55	7.5	0.9775	321.35	9.6	0.9796	306.05	7.09
0.9939	312.35	7.47	0.9775	322.25	8.99	0.9796	308.05	7.41
0.9939	312.05	7.42	0.9775	322.45	9.89	0.9796	307.85	7.32
0.9939	317.35	8.15	0.9775	322.45	9.58	0.9796	307.75	7.33
0.9939	317.75	8.2	0.9775	328.05	11.7	0.9796	310.75	7.8
0.9939	317.05	8.15	0.9775	327.95	11.14	0.9796	311.85	8.26
0.9939	317.05	8.27	0.9775	327.95	11.47	0.9796	312.25	8
0.9939	321.75	8.74	0.9775	327.35	10.98	0.9796	312.45	8.06
0.9939	322.75	8.58	0.9810	306.85	7.4	0.9796	317.55	9.15
0.9939	322.85	8.67	0.9810	308.25	7.64	0.9796	317.65	9.06
0.9939	322.65	8.75	0.9810	306.65	7.2	0.9796	318.85	9
0.9939	326.55	9.48	0.9810	309.25	7.6	0.9796	318.45	8.92
0.9939	327.05	9.37	0.9810	312.45	7.77	0.9796	322.85	10.18
0.9939	327.75	9.35	0.9810	314.15	8.15	0.9796	322.05	9.97
0.9939	326.95	9.23	0.9810	312.75	8.09	0.9796	321.05	9.93
0.9948	305.35	7.09	0.9810	312.35	8.21	0.9796	321.95	9.98
0.9948	306.25	7.19	0.9810	317.15	8.34	0.9796	326.85	11.05
0.9948	307.15	7.21	0.9810	317.75	8.82	0.9796	327.55	10.84
0.9948	306.85	7.13	0.9810	317.25	8.17	0.9796	326.85	11.26
0.9948	311.35	7.61	0.9810	316.35	8.88	0.9796	327.75	10.58
0.9948	312.65	7.62	0.9810	322.15	9.72	0.9938	306.45	7.25
0.9948	312.35	7.74	0.9810	322.95	9.95	0.9938	307.35	7.22
0.9948	312.75	7.58	0.9810	322.45	10.19	0.9938	307.85	7.36

0.9948	317.55	8.3	0.9810	322.75	10.39	0.9938	308.35	7.36
0.9948	317.35	8.07	0.9810	327.05	10.95	0.9938	310.65	7.73
0.9948	317.65	8.01	0.9810	328.55	11.39	0.9938	313.25	7.7
0.9948	317.55	8.11	0.9810	327.55	11.6	0.9938	312.35	7.62
0.9948	322.05	8.78	0.9810	327.75	12.22	0.9938	312.05	7.65
0.9948	322.85	8.73	0.9988	306.85	7.19	0.9938	315.45	8.24
0.9948	321.95	8.77	0.9988	307.45	7.25	0.9938	313.65	8.39
0.9948	321.05	8.78	0.9988	306.35	7.27	0.9938	315.75	8.45
0.9948	328.45	9.46	0.9988	308.05	7.14	0.9938	316.05	8.29
0.9948	327.65	9.37	0.9988	311.25	7.57	0.9938	322.55	9.07
0.9948	327.25	9.63	0.9988	312.85	7.6	0.9938	322.95	9.04
0.9948	327.95	9.4	0.9988	312.25	7.55	0.9938	323.55	9.04
			0.9988	311.95	7.56	0.9938	322.85	9.06
			0.9988	315.65	8.08	0.9938	327.15	9.39
			0.9988	317.75	8.29	0.9938	327.65	9.61
			0.9988	316.95	8.12	0.9938	327.65	9.59
			0.9988	317.95	8.3	0.9938	326.55	9.46
			0.9988	322.25	8.89			
			0.9988	322.55	8.98			
			0.9988	322.55	9.16			
			0.9988	322.95	9.17			
			0.9988	327.75	9.62			
			0.9988	327.35	9.53			
			0.9988	326.75	9.56			
			0.9988	326.25	9.47			
			0.9988	307.75	7.39			
			0.9988	307.45	7.24			
			0.9988	307.55	7.34			
			0.9988	307.95	7.29			
			0.9988	311.85	7.66			
			0.9988	312.75	7.67			
			0.9988	312.65	7.63			
			0.9988	312.65	7.57			
			0.9988	317.45	8.25			
			0.9988	317.95	8.15			
			0.9988	318.25	8.14			
			0.9988	322.55	8.92			
			0.9988	322.85	8.83			
			0.9988	323.25	9.01			
			0.9988	327.85	9.71			
			0.9988	328.05	9.71			
			0.9988	327.95	9.56			

7.3. Laboratory measurements. Redissolution Points.

Table 17. Laboratory raw data. Redissolution points. Bold Type: Data included in Aspen.

1:1 Acet/Isop.			3:1 Acet/Isop.			5:1 Acet/Isop		
x_CO$_2$	T[K]	P[MPa]	x_CO$_2$	T[K]	P[MPa]	x_CO$_2$	T[K]	P[MPa]
0.7118	308.95	5.71	0.7668	308.75	5.96	**0.7129**	**308.85**	**5.37**
0.7118	**306.95**	**5.84**	**0.7668**	**309.45**	**5.62**	0.7129	309.05	5.47
0.7118	**309.45**	**6**	**0.7668**	**309.25**	**5.75**	0.7129	308.95	5.36
0.7118	313.85	6.26	0.7668	310.85	6.28	0.7129	308.95	5.46
0.7118	314.15	6.59	0.7668	314.15	6.54	**0.7129**	**314.95**	**6.63**
0.7118	313.95	6.14	0.7668	315.55	7.1	0.7129	314.85	6.25
0.7118	319.25	6.72	0.7668	315.45	7.16	0.7129	316.85	6.83
0.7118	320.15	7.13	**0.7668**	**314.65**	**6.32**	0.7129	319.55	6.59
0.7118	319.35	7.02	0.7668	322.15	8.75	0.7129	320.55	6.84
0.7118	324.25	7.97	0.7668	319.65	7.86	0.7129	318.65	6.32
0.7118	**324.75**	**7.47**	0.7668	321.55	8.58	0.7129	323.75	6.76
0.7118	**324.85**	**7.59**	**0.7668**	**319.95**	**7.43**	0.7129	324.95	6.96
0.7118	324.55	7.62	0.7668	323.65	7.82	0.7129	323.35	6.66
0.7118	327.75	7.85	0.7668	326.65	8.21	0.7129	323.45	6.92
0.7118	330.15	8.21	0.7668	325.05	7.91	0.7129	329.45	8.25
0.7491	312.55	7.23	0.7668	325.45	7.75	0.7129	329.85	8.03
0.7491	310.15	6.56	**0.7668**	**330.25**	**8.23**	0.7129	330.85	8.28
0.7491	312.45	6.94	0.7668	329.45	8.44	0.7499	309.85	5.6
0.7491	**311.35**	**6.35**	0.7668	329.35	8.52	0.7499	309.35	5.69
0.7491	**314.45**	**6.67**	0.7668	328.95	8.46	0.7499	309.95	5.58
0.7491	**314.75**	**6.64**	0.7927	310.15	6.24	0.7499	315.25	7.32
0.7491	**313.95**	**6.43**	**0.7927**	**310.65**	**6.02**	0.7499	314.85	7.17
0.7491	**315.15**	**6.62**	0.7927	310.75	6.48	0.7499	315.05	6.71
0.7491	320.45	7.4	**0.7927**	**310.55**	**6.32**	0.7499	320.55	8.08
0.7491	319.45	7.27	0.7927	312.65	7.1	0.7499	320.75	8.13
0.7491	318.95	6.9	0.7927	314.95	7.66	0.7499	319.85	8.4
0.7491	319.55	7.55	0.7927	315.05	7.42	0.7499	325.25	7.32
0.7491	323.15	7.66	**0.7927**	**314.65**	**7.42**	0.7499	324.55	7.37
0.7491	324.25	7.44	0.7927	320.65	7.55	0.7499	325.25	7.86
0.7491	323.55	7.63	0.7927	318.95	7.29	0.7499	328.75	7.91
0.7491	323.65	7.48	0.7927	321.55	7.89	0.7499	331.45	8.16
0.7491	328.65	7.76	0.7927	319.35	7.64	0.7499	329.05	8.04
0.7491	329.15	7.94	0.7927	324.15	7.44	0.8961	307.95	6.76
0.7491	328.65	7.86	0.7927	327.35	8.59	**0.8961**	**308.75**	**6.61**
0.7491	329.65	8.23	0.7927	323.95	7.9	0.8961	309.35	6.94
0.8930	310.75	7.51	0.7927	324.05	7.98	0.8961	313.75	7.67
0.8930	309.65	7.01	0.7927	330.85	8.49	0.8961	315.45	7.79
0.8930	309.75	7.16	0.7927	329.65	8.16	0.8961	314.95	7.55
0.8930	317.25	7.82	0.7927	329.05	8.17	0.8961	320.65	8.37
0.8930	314.55	7.47	0.7927	328.65	8.69	0.8961	320.95	9.52
0.8930	314.25	7.66	0.9052	310.35	7.2	0.8961	319.55	9.48
0.8930	318.65	8.05	0.9052	311.15	7.12	0.8961	323.45	10.16

0.8930	319.15	8.02	**0.9052**	**309.85**	**7.11**	0.8961	324.15	10.21
0.8930	318.75	8.02	0.9052	311.15	7.54	0.8961	324.65	9.9
0.8930	325.85	9.93	0.9052	315.05	7.87	0.8961	329.65	10.76
0.8930	324.65	9.69	0.9052	313.95	7.87	0.8961	329.55	10.62
0.8930	326.55	10.08	0.9052	315.45	7.42	0.8961	329.65	10.51
0.8930	331.35	10.68	0.9052	314.65	7.64	0.8961	329.95	10.03
0.8930	328.85	10.64	0.9052	319.55	7.98	0.9100	308.25	6.85
0.8930	329.25	10.6	0.9052	319.85	8.54	0.9100	308.85	6.97
0.9351	310.25	8.14	0.9052	319.45	8.35	0.9100	309.05	6.92
0.9351	311.25	8.28	0.9052	318.75	7.91	0.9100	315.05	7.99
0.9351	310.15	8.02	0.9052	323.85	8.62	0.9100	314.25	7.61
0.9351	313.25	8.58	0.9052	323.05	8.74	0.9100	314.35	7.78
0.9351	315.85	8.33	0.9052	324.55	9.07	0.9100	319.55	8.32
0.9351	314.45	8.32	0.9052	329.55	9.68	0.9100	320.55	8.19
0.9351	318.65	9.07	0.9052	330.25	9.74	0.9100	318.65	8.32
0.9351	319.65	9.36	0.9052	329.25	9.69	**0.9100**	**323.65**	**9.15**
0.9351	318.85	9.26	0.9052	330.15	9.63	0.9100	323.95	9.06
0.9351	324.15	9.6	0.9181	308.05	7.16	0.9100	323.95	9.07
0.9351	324.25	9.52	0.9181	308.45	7.39	0.9100	329.55	10.83
0.9351	324.15	9.24	0.9181	310.15	7.68	0.9100	328.85	10.18
0.9351	329.35	10.05	0.9181	318.95	8.28	0.9100	328.85	11.04
0.9351	329.45	9.93	0.9181	316.65	8.39	0.9100	328.95	10.55
0.9351	331.55	10.1	0.9181	316.55	8.1	0.9368	308.75	7.39
0.9444	308.85	8.26	0.9181	320.75	8.69	0.9368	309.35	7.08
0.9444	309.25	8.15	0.9181	320.45	8.61	0.9368	308.75	7.19
0.9444	309.95	8.04	0.9181	320.05	8.53	0.9368	309.55	7.16
0.9444	313.55	8.22	0.9181	326.25	9.99	0.9368	307.95	7.08
0.9444	313.95	8.66	0.9181	324.45	10.25	0.9368	313.65	7.66
0.9444	314.35	8.47	0.9181	325.75	10.66	0.9368	314.85	8.26
0.9444	319.45	8.77	0.9181	328.95	11.32	0.9368	313.65	7.73
0.9444	317.65	8.35	0.9181	329.45	11.27	0.9368	314.15	7.94
0.9444	320.15	8.98	0.9181	330.25	11.93	0.9368	319.95	9.07
0.9444	325.35	9.82	0.9512	309.35	7.77	0.9368	319.75	8.89
0.9444	326.25	9.99	0.9512	309.65	7.52	0.9368	319.05	8.56
0.9444	324.15	9.47	0.9512	309.65	7.86	0.9368	319.45	8.72
0.9444	331.05	10.29	0.9512	310.65	7.94	0.9368	324.35	9.35
0.9444	332.05	10.27	0.9512	314.85	8.86	0.9368	324.05	9.57
0.9444	332.25	10.33	0.9512	316.35	9.07	0.9368	324.05	9.9
0.9798	308.65	7.49	0.9512	315.25	8.42	0.9368	324.85	10.03
0.9798	309.55	7.48	0.9512	315.65	8.48	0.9368	330.25	11.09
0.9798	309.05	7.4	0.9512	319.05	9.86	0.9368	328.45	10.58
0.9798	310.45	7.15	0.9512	320.75	9.72	0.9368	328.85	10.44
0.9798	313.55	8.04	0.9512	322.45	9.89	0.9368	329.85	10.67
0.9798	315.05	8.4	0.9512	320.15	9.59	0.9454	308.35	7.34
0.9798	314.65	8.21	0.9512	326.35	10.73	0.9454	310.65	7.79
0.9798	315.05	8.48	0.9512	324.25	10.17	0.9454	311.05	7.98

0.9798	320.15	8.96	0.9512	325.25	10.18	0.9454	310.75	7.87
0.9798	318.55	8.63	0.9512	325.45	10.12	0.9454	314.15	8.89
0.9798	318.75	8.79	0.9512	331.25	11.07	0.9454	317.05	8.81
0.9798	318.45	8.53	0.9512	331.05	10.84	0.9454	315.95	8.8
0.9798	323.15	9.04	0.9512	330.75	10.81	0.9454	315.85	9.06
0.9798	323.35	9.11	0.9512	331.35	10.86	0.9454	319.05	9.32
0.9798	325.45	9.89	0.9570	310.85	7.98	0.9454	319.15	9.28
0.9798	324.35	9.5	0.9570	309.35	7.79	0.9454	319.05	8.87
0.9798	328.85	9.84	0.9570	309.65	7.85	0.9454	319.25	9.19
0.9798	328.95	9.77	0.9570	309.45	7.81	0.9454	323.95	10.25
0.9798	328.45	9.6	0.9570	315.05	8.76	0.9454	323.95	9.98
0.9798	328.65	9.82	0.9570	314.95	8.87	0.9454	323.65	9.81
0.9822	308.85	7.5	0.9570	315.95	9.03	0.9454	325.05	9.75
0.9822	309.65	7.49	0.9570	316.05	8.65	0.9454	328.65	10.9
0.9822	308.95	7.48	0.9570	321.25	9.96	0.9454	329.95	10.99
0.9822	310.65	7.23	0.9570	322.45	9.93	0.9454	331.75	10.61
0.9822	315.95	8.34	0.9570	322.45	10.45	0.9454	328.45	10.53
0.9822	314.65	7.79	0.9570	321.85	10.06	0.9759	308.65	7.56
0.9822	313.95	7.84	0.9570	324.75	10.07	0.9759	309.05	7.61
0.9822	315.35	8.22	0.9570	324.75	10.14	0.9759	309.15	7.49
0.9822	320.45	8.94	0.9570	323.85	10.37	0.9759	309.45	7.65
0.9822	319.25	8.72	0.9570	323.15	10.24	0.9759	315.35	8.49
0.9822	318.55	8.72	0.9570	331.45	10.82	0.9759	315.85	8.48
0.9822	318.55	8.53	0.9570	328.55	11.43	0.9759	316.75	8.73
0.9822	324.45	9.59	0.9570	328.55	10.75	0.9759	316.75	8.55
0.9822	323.75	9.43	0.9570	330.25	11.1	0.9759	319.45	8.89
0.9822	324.05	9.66	0.9775	310.25	7.44	0.9759	319.95	9.08
0.9822	323.85	9.75	0.9775	311.05	7.51	0.9759	319.65	9.12
0.9822	328.35	10.11	0.9775	311.65	7.3	0.9759	319.15	9.15
0.9822	328.55	9.75	0.9775	306.05	7.28	0.9759	323.85	10.04
0.9822	329.35	9.94	0.9775	315.35	8.15	0.9759	324.55	10.55
0.9822	328.85	10.06	0.9775	314.35	7.73	0.9759	325.75	10.63
0.9939	306.25	7.65	0.9775	314.75	7.98	0.9759	324.05	10.1
0.9939	309.75	7.31	0.9775	314.25	7.61	0.9759	328.45	10.66
0.9939	307.35	7.36	0.9775	318.25	8.31	0.9759	328.85	11.16
0.9939	307.55	7.58	0.9775	319.65	9.29	0.9759	328.65	11.64
0.9939	313.35	7.84	0.9775	322.15	9.98	0.9759	328.55	11.19
0.9939	315.45	7.94	0.9775	329.45	10.98	0.9796	309.95	7.77
0.9939	314.75	7.77	0.9775	328.05	11.03	0.9796	312.25	8.15
0.9939	315.35	7.9	0.9775	323.45	10.45	0.9796	312.95	8.81
0.9939	318.15	8.57	0.9775	323.25	10.71	0.9796	313.35	8.63
0.9939	318.85	8.53	0.9775	329.05	12.43	0.9796	313.75	8.5
0.9939	317.85	8.54	0.9775	329.15	12.43	0.9796	313.95	8.83
0.9939	318.45	8.72	0.9775	327.85	12.49	0.9796	316.45	8.9
0.9939	324.65	8.64	0.9775	328.65	12.2	0.9796	314.55	8.68
0.9939	325.45	8.58	0.9810	310.85	7.45	0.9796	321.25	9.28

Table 17. Laboratory raw data. Redissolution points. Bold Type: Data included in Aspen (4/5)

0.9939	323.55	9.17	0.9810	311.75	7.95	0.9796	318.85	9.55
0.9939	322.95	8.92	0.9810	312.25	7.98	0.9796	318.45	9.24
0.9939	328.25	9.92	0.9810	311.45	7.78	0.9796	318.75	9.58
0.9939	328.45	9.67	0.9810	316.45	8.36	0.9796	324.35	10.82
0.9939	328.45	9.67	0.9810	314.95	7.75	0.9796	324.45	11.46
0.9939	328.25	9.43	0.9810	316.55	8.4	0.9796	323.85	11.27
0.9948	309.25	7.83	0.9810	314.05	7.94	0.9796	324.05	11.28
0.9948	309.65	8.36	0.9810	322.45	9.48	0.9796	329.15	11.74
0.9948	310.65	7.94	0.9810	322.95	9.44	0.9796	329.05	12.13
0.9948	309.95	7.56	0.9810	323.95	10.25	0.9796	330.45	11.61
0.9948	313.05	7.92	0.9810	320.35	9.4	0.9796	330.65	12.31
0.9948	315.45	8.23	0.9810	323.85	10.92	0.9938	311.05	7.45
0.9948	314.25	7.95	0.9810	323.85	10.95	0.9938	309.65	7.51
0.9948	314.35	8.03	0.9810	323.55	11.38	0.9938	309.65	7.45
0.9948	318.25	8.51	0.9810	323.35	11.47	0.9938	309.95	7.39
0.9948	319.75	8.53	0.9810	328.75	11.85	0.9938	313.55	7.75
0.9948	318.75	8.31	0.9810	328.95	12.32	0.9938	315.95	8.47
0.9948	318.05	8.44	0.9810	328.35	12.9	0.9938	313.65	8.23
0.9948	323.25	9.29	0.9810	328.95	14.09	0.9938	314.45	8.09
0.9948	324.05	9.28	0.9988	308.55	7.45	0.9938	318.95	8.31
0.9948	323.25	9.24	0.9988	310.35	7.51	0.9938	317.45	8.83
0.9948	322.65	9.13	0.9988	309.95	7.36	0.9938	317.65	8.64
0.9948	328.45	9.59	0.9988	310.55	7.61	0.9938	319.45	8.66
0.9948	327.95	9.66	0.9988	313.45	7.71	0.9938	323.15	9.15
0.9948	328.35	9.37	0.9988	314.45	7.99	0.9938	324.15	9.03
0.9948	328.45	9.72	0.9988	313.85	7.83	0.9938	323.85	8.93
			0.9988	314.15	7.97	0.9938	323.05	9.05
			0.9988	318.25	8.66	0.9938	328.65	9.39
			0.9988	318.45	8.53	0.9938	328.95	9.86
			0.9988	320.55	8.67	0.9938	328.55	9.79
			0.9988	318.35	8.48	0.9938	328.25	9.44
			0.9988	324.05	8.89			
			0.9988	322.95	8.98			
			0.9988	324.05	9.16			
			0.9988	323.65	9.17			
			0.9988	328.15	9.88			
			0.9988	328.15	10.03			
			0.9988	328.85	10.28			
			0.9988	328.95	9.96			
			0.9988	309.05	7.39			
			0.9988	308.85	7.24			
			0.9988	308.65	7.34			
			0.9988	309.15	7.29			
			0.9988	313.45	7.92			
			0.9988	313.75	7.9			
			0.9988	313.85	7.95			

Table 17. Laboratory raw data. Redissolution points. Bold Type: Data included in Aspen (5/5)

0.9988	313.65	7.85
0.9988	318.65	8.34
0.9988	318.75	8.22
0.9988	319.25	8.41
0.9988	322.75	9.02
0.9988	324.25	9.03
0.9988	323.15	9.08
0.9988	330.65	9.98
0.9988	328.35	9.72
0.9988	328.35	9.9